FREEZING MULTIPULSES AND MULTIFRONTS

WOLF-JÜRGEN BEYN*, SABRINA SELLE*, VERA THÜMMLER*

FAKULTÄT FÜR MATHEMATIK, UNIVERSITÄT BIELEFELD

POSTFACH 100131, D-33501 BIELEFELD

Abstract. We consider nonlinear time dependent reaction diffusion systems in one space dimension that exhibit multiple pulses or multiple fronts. In an earlier paper two of the authors developed the freezing method that allows to compute a moving coordinate frame in which, for example, a traveling wave becomes stationary. In this paper we extend the method to handle multifronts and multipulses traveling at different speeds. The solution of the Cauchy problem is decomposed into a finite number of single waves each of which has its own moving coordinate system. The single solutions satisfy a system of partial differential algebraic equations coupled by nonlinear and nonlocal terms. Applications are provided to the Nagumo and the FitzHugh-Nagumo system. We justify the method by showing that finitely many traveling waves, when patched together in an appropriate way, solve the coupled system in an asymptotic sense. The method is generalized to equivariant evolution equations and illustrated by the complex Ginzburg Landau equation.

Key words. Multipulses, partial differential algebraic equations, unbounded domains, equivariance, Lie groups

AMS subject classifications. 65M99, 35K57

1. Introduction. Consider a parabolic system for a function $u(x,t) \in \mathbb{R}^m$ on the real line

$$u_t = Au_{xx} + f(u, u_x), \quad x \in \mathbb{R}, t \geq 0, \quad u(x,0) = u_0(x), \ x \in \mathbb{R}, \qquad (1.1)$$

where $A \in \mathbb{R}^{m,m}$ is assumed to be positive definite and $f : \mathbb{R}^{2m} \to \mathbb{R}^m$ is assumed to be smooth. We are interested in systems that have more than one traveling wave solution

$$u_j(x,t) = w_j(x - c_j t), \quad j = 1, \ldots, N \qquad (1.2)$$

traveling at different speeds c_j and with limiting behavior

$$w_j^- = \lim_{\xi \to -\infty} w_j(\xi), \quad w_j^+ = \lim_{\xi \to \infty} w_j(\xi). \qquad (1.3)$$

It is frequently observed that such systems exhibit special solutions that look like a superposition of several waves. In Figure 1.1 we illustrate the case of two pulses and two fronts that travel in opposite direction ($c_1 < 0 < c_2$) and that can be patched together (i.e. $w_1^+ = w_2^-$), see Section 2 for a more precise definition of the meaning of patching. Solutions of this type are usually called multifronts or multipulses depending on whether the limits at $\pm\infty$ agree or disagree. There is quite an extensive literature that studies existence and stability of multifronts and multipulses close to a fixed pulse configuration with the single pulses far apart and with a common speed, see [15], [13], [14], [16], [22], [6]. More recently, in [23] a center manifold is constructed that contains all types of multipulses (even infinitely many) with large spacings that travel at a slowly varying speed.

In this paper we consider a finite number of pulses resp. fronts that travel at different speeds. We provide a working definition for multifront solutions in an asymptotic sense that will be sufficient for our approach. Note that in the recent paper [17] the

---
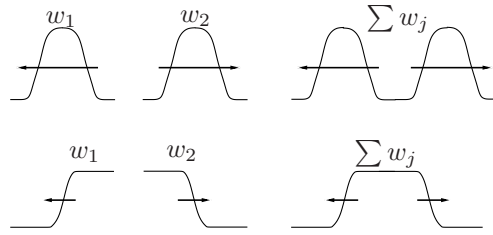
FIG. 1.1. *Single pulses/multipulse and single fronts/multifront*

authors construct an invariant manifold that contains and attracts such solutions up to a certain time instance prior to collision.

The main goal of this paper is to numerically construct a decomposition of the solution $u(x, t)$ of the Cauchy problem (1.1) of the form

$$u(x, t) = \sum_{j=1}^{N} v_j(x - g_j(t), t). \tag{1.4}$$

The idea is to find functions $v_j : \mathbb{R} \times [0, \infty) \to \mathbb{R}^m$, $(\xi, t) \mapsto v_j(\xi, t)$ that approximate the j−th profile in the multifront and that have a rather local support when compared to the overall solution $u(x, t)$. The functions $g_j : \mathbb{R} \to \mathbb{R}$ denote the time-dependent position of the j-th profile and will be determined by the numerical process as well. The N-dimensional system that determines the v_j will be set up such that the linear superposition (1.4) is an exact solution of the nonlinear system (1.1) and such that this system can be solved on a much smaller domain than the original equation. Note that, if repelling pulses or fronts appear as in Figure 1.1, then growing spatial domains are needed to compute and represent the solution of (1.1), while our system will be solved on a domain of moderate size that stays constant for all times. Moreover, our method will produce the individual velocities automatically without any a-posteriori analysis of simulation data.

We follow the freezing approach for single waves in [3],[4] (see [12] for a related approach) by setting up an appropriate phase condition for each of the single profiles v_j. In Section 2 we derive the basic system of N partial differential algebraic equations (PDAEs) for the functions v_j that will be solved numerically. The nonlinearities in this system contain nonlocal terms due to the different positions of the single profiles.

For the numerical computations we truncate this system to a finite interval, use appropriate boundary conditions, and discretize by finite elements in space and BDF methods in time. In Section 3 we show several applications of our method to multi-fronts that occur in the Nagumo and in the FitzHugh-Nagumo system. It may come as a surprise that the method even works in cases for which it was not designed, namely fronts or pulses that collide and annihilate each other.

In Section 4 we give a certain theoretical justification of our method. It is shown that appropriately modified waves (1.2) satisfy the PDAE system in an asymptotic sense.

Finally, in Section 5 we generalize our 'decompose and freeze' approach to general evolution equations that are equivariant with respect to the action of a (not necessarily compact) Lie group. As an application we discuss the decomposition of solutions of a complex Ginzburg Landau equation that has a two dimensional group of equivariances.

2. Decomposition of Multifronts. Let us be more precise about the process of patching single waves (1.2). Assume that the left and right limits of the waves match in the sense that

$$w_j^+ = w_{j+1}^-, \quad j = 1, \ldots, N - 1. \tag{2.1}$$

Then we write down the superposition

$$U(x,t) = \sum_{j=1}^{N} \hat{w}_j(x - c_j t), \quad \hat{w}_j(\xi) = \left\{ \begin{array}{ll} w_1(\xi) & j = 1 \\ w_j(\xi) - w_j^- & j \geq 2 \end{array} \right. , \tag{2.2}$$

where we have subtracted left limits so that the modified profiles $\hat{w}_j$, cf. Figure 2.1, fit together upon summation. In particular, this guarantees by (2.1)

$$\lim_{x \to \infty} u(x,t) = \sum_{j=1}^{N} w_j^+ - \sum_{j=2}^{N} w_j^- = w_N^+. \tag{2.3}$$
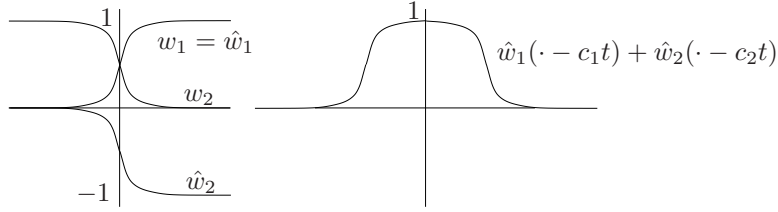

FIG. 2.1. *The modified profiles $\hat{w}_j$, asymptotic 2-front solution $\hat{w}_1(x - c_1 t) + \hat{w}_2(x - c_2 t)$ at $t > 0$, $c_1 < 0 < c_2$*

In Section 4 we will show that $U(x,t)$ defined by (2.2) satisfies (1.1) in an asymptotic sense, i.e.

$$\|U_t - (AU_{xx} + f(U, U_x))\| \to 0 \ \text{ as } t \to \infty \tag{2.4}$$

for some suitable norm $\| \cdot \|$, e.g. the $\mathcal{L}_2$-norm.

Our goal is to set up a decomposition (1.4) that approaches the form (2.2) in an asympotic sense.

We use a bump function $\varphi \in C^\infty(\mathbb{R}, \mathbb{R})$ that satisfies

$$0 < \varphi(x) \leq C \quad \forall x \in \mathbb{R} \tag{2.5}$$

and has its main mass located near zero. The precise form of φ is not important, but we mention that both, numerical computation and the theory in Section 4, work for exponential decay of type $\varphi(t) \asymp e^{-\beta|x|^k}, \beta > 0, \ k \geq 1$.

We look for a solution of the form (1.4) and insert this into equation (1.1). We suppress the arguments $(x - g_j(t), t)$ of v_j and find

$$\begin{aligned}
u_t &= \sum_{j=1}^{N} [v_{j,t} - v_{j,\xi} g_{j,t}] \\
&= \sum_{j=1}^{N} A v_{j,\xi\xi} + f\left(\sum_{k=1}^{N} v_k, \sum_{k=1}^{N} v_{k,\xi} \right) \\
&= \sum_{j=1}^{N} \left[A v_{j,\xi\xi} + \frac{\varphi(\cdot - g_j(t))}{\sum_{k=1}^{N} \varphi(\cdot - g_k(t))} f\left(\sum_{k=1}^{N} v_k, \sum_{k=1}^{N} v_{k,\xi} \right) \right].
\end{aligned} \tag{2.6}$$

Note that the quotients

$$\frac{\varphi(x - g_j(t))}{\sum_{k=1}^{N} \varphi(x - g_k(t))} \tag{2.7}$$

form a time-dependent partition of unity and that the denominator never vanishes due to (2.5). In (2.6) we have used this partition to localize the nonlinear part of the vector field but not the solutions themselves.

A sufficient condition for (2.6) to hold is that each of the terms in brackets vanishes. Substituting $\xi = x - g_j(t)$ and $\mu_j = g_{j,t}$ leads to the following system of N coupled PDEs for $\xi \in \mathbb{R}, t \geq 0$.

$$v_{j,t}(\xi, t) = A v_{j,\xi\xi}(\xi, t) + v_{j,\xi}(\xi, t)\mu_j(t) + \frac{\varphi(\xi)}{\sum_{k=1}^{N} \varphi(\xi - g_k + g_j)}$$
$$\cdot f\left(\sum_{k=1}^{N} v_k(\xi - g_k + g_j, t), \sum_{k=1}^{N} v_{k,\xi}(\xi - g_k + g_j, t)\right), \quad j = 1, \ldots, N \tag{2.8}$$

and the simple set of ODEs

$$g_{j,t} = \mu_j(t), \quad j = 1, \ldots, N. \tag{2.9}$$

In the following it will be convenient to write $v = (v_1, \ldots, v_N)$, $g = (g_1, \ldots, g_N)$, $\mu = (\mu_1, \ldots, \mu_N)$ and to abbreviate terms in (2.8)

$$F_j(v, g)(\xi, t) = Q_j^g(\xi, t) f\left(\sum_{k=1}^{N} v_k(\xi_{kj}^g, t), \sum_{k=1}^{N} v_{k,\xi}(\xi_{kj}^g, t)\right),$$
$$Q_j^g(\xi, t) = \frac{\varphi(\xi)}{\sum_{k=1}^{N} \varphi(\xi_{kj}^g)}, \qquad \xi_{kj}^g = \xi - g_k(t) + g_j(t). \tag{2.10}$$

We note that the nonlinear terms $F_j(v, g)$ couple the single functions $v_k, k = 1, \ldots, N$ in a nonlocal fashion. From the derivation we also see that one can allow $j-$dependent bump functions φ_j that take the size of the $j-$th profile into account. The quotient in (2.7) then reads

$$\frac{\varphi_j(x - g_j(t))}{\sum_{k=1}^{N} \varphi_k(x - g_k(t))}. \tag{2.11}$$

The system will be completed by initial conditions for v_j, g_j and by phase conditions that compensate for the extra unknowns μ_j.
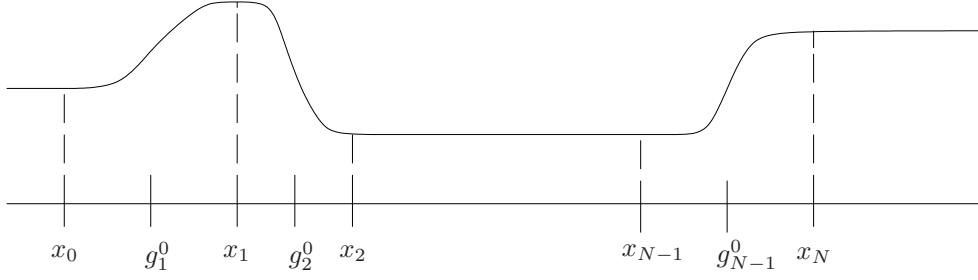
We impose initial conditions

$$v_j(\xi, 0) = v_j^0(\xi), \quad \xi \in \mathbb{R}, j = 1, \ldots, N \tag{2.12}$$

$$g_j(0) = g_j^0, \quad j = 1, \ldots, N \tag{2.13}$$

that should satisfy

$$u_0(x) = \sum_{j=1}^{N} v_j^0(x - g_j^0), \quad x \in \mathbb{R}. \tag{2.14}$$

FIG. 2.2. *Decomposition of the initial data u_0.*

In most of our applications below we first select v_j^0, g_j^0 and then define u_0 by (2.14). If, on the other hand, u_0 is given then one has to do some surgery for finding appropriate values for v_j^0 and g_j^0. Assume, for example, that a function u_0 is given that forms plateaus near points $x_0 < x_1 < \ldots, x_N$ (see Figure 2.2). Then one may choose $g_j^0 = \frac{1}{2}(x_{j-1} + x_j)$ for $j = 1, \ldots, N$ and similar to (2.2) define

$$v_j^0(\xi) = -u_0(x_{j-1}) + \begin{cases} u_0(x_{j-1}), & \xi + g_j^0 \le x_{j-1} \\ u_0(\xi + g_j^0), & x_{j-1} \le \xi + g_j^0 \le x_j \qquad j = 2, \ldots, N-1 \\ u_0(x_j), & x_j \le \xi + g_j^0, \end{cases}$$

and

$$v_1^0(\xi) = \begin{cases} u_0(\xi + g_1^0), & \xi + g_1^0 \le x_1 \\ u_0(x_1), & x_1 \le \xi + g_1^0, \end{cases}$$

$$v_N^0(\xi) = \begin{cases} 0, & \xi + g_N^0 \le x_{N-1} \\ u_0(\xi + g_N^0) - u_0(x_{N-1}), & x_{N-1} \le \xi + g_N^0. \end{cases}$$

Next we discuss the choice of phase condition that will make the solution of the system (2.8),(2.9),(2.13),(2.14) unique. For the case of freezing single waves two possibilities were suggested in [3],[4].

First, suppose that we have template functions $\hat{v}_j$ (e.g. $\hat{v}_j = v_j^0$) to which we would like the v_j to stay as close as possible. This requires the distance $d_j(g) = \|v_j(\cdot, t) - \hat{v}_j(\cdot - g)\|_{\mathcal{L}^2}$ to achieve its minimum at $g = 0$ for all times. Differentiating with respect to g yields the necessary conditions

$$\langle v_j - \hat{v}_j, \hat{v}_{j,\xi} \rangle_{\mathcal{L}^2} = 0, \quad j = 1, \ldots, N. \tag{2.15}$$

In the terminology of differential algebraic equations this constraint leads to an index 2 problem. If we differentiate (2.15) with respect to t and use (2.8) we have

$$\psi_{\mathrm{fix}}(v, \mu) = (\mu_j \langle \hat{v}_{j,\xi}, v_{j,\xi} \rangle_{\mathcal{L}^2} + \langle \hat{v}_{j,\xi}, A v_{j,\xi\xi} + F_j(v, g) \rangle_{\mathcal{L}^2})_{j=1}^N = 0. \tag{2.16}$$

If $\langle \hat{v}_{j,\xi}, v_{j,\xi} \rangle_{\mathcal{L}^2} \ne 0$ then we can determine μ_j from this equation and thus have reduced the problem to index 1.

Second, choose the values μ_j so that $v_{j,t}$ in (2.8) is minimized at each time instance. Geometrically this requires that the time derivative $v_{j,t}(\cdot, t)$ is orthogonal to the group orbit $\{v_j(\cdot - g, t) : g \in \mathbb{R}\}$ at all times. This leads to the phase condition

$$\psi_{\mathrm{orth}}(v, \mu) = (\langle v_{j,\xi}, v_{j,t} \rangle_{\mathcal{L}^2})_{j=1}^N = (\langle v_{j,\xi}, A v_{j,\xi\xi} + \mu_j v_{j,\xi} + F_j(v, g) \rangle_{\mathcal{L}^2})_{j=1}^N = 0, \tag{2.17}$$

which allows to solve for μ_j whenever $v_{j,\xi}$ is nonconstant. Note that (2.17) can be obtained from (2.16) when replacing $\hat{v}_{j,\xi}$ by $v_{j,\xi}$. The complete system to be solved is now given by the PDAE (2.8), (2.9), (2.12), (2.13) with either (2.16) or (2.17) as phase condition.

The relative merits of both types of conditions have been discussed for the single freezing in [3],[20]. It was shown in [20],[19] that the fixed phase conditions leads to a well-posed PDAE in the neighborhood of a relative equilibrium in one space dimension. Moreover, the PDAE as well as its discretization on a finite interval have the wave and its velocity as an asymptotically stable steady state in the classical Liapunov sense. In [4] we have shown that this pertains on the continuous level to the orthogonality constraint (2.17). Locally near relative equilibria there is not much of a difference between both conditions. It is hard to make a general statement for more global situations, when the initial data are far from any equilibrium. Generally, the orthogonality condition is more flexible globally since it requires to pre-knowledge of the solution, whereas the fixed phase condition tends to lead to PDAEs with a better conditioning.

We conclude with some remarks concerning the numerical solution of the PDAE system. In Section 3 we will discretize the PDAE as a whole by conventional methods. It is clear that the effort of solving the system grows linearly with the number of pulses or fronts present in the solution. On the other hand, in contrast to the original equation, one can solve the PDAE system on a fixed and relatively small spatial domain. So far, the interaction terms that need values outside this domain were calculated by extrapolating with constant boundary values. One may think of reducing the spatial domain further by solving linearized equations (explicitly) in the outside domain and using this for calculating the interaction. We have not yet pursued the details of such an extension. A method of this type will be reminiscent of the vortex blob method in fluid dynamics (see [2], [8]) which follows moving vortices and then uses the Biot-Savart law for treating interactions.

3. Applications. We illustrate the method on two examples which possess traveling fronts and pulses: the Nagumo and the FitzHugh-Nagumo equations which both model nerve conduction.

For two components the PDAE (2.8),(2.9) with the phase fixing condition (2.16) reads

$$v_{1,t} = Av_{1,\xi\xi} + v_{1,\xi}\mu_1(t) + \frac{\varphi(\cdot)}{\varphi(\cdot) + \varphi(\cdot - g_2 + g_1)}f(v_1(\cdot,t) + v_2(\cdot - g_2 + g_1, t))$$

$$v_{2,t} = Av_{2,\xi\xi} + v_{2,\xi}\mu_2(t) + \frac{\varphi(\cdot)}{\varphi(\cdot) + \varphi(\cdot - g_1 + g_2)}f(v_2(\cdot,t) + v_1(\cdot - g_1 + g_2, t)) \quad (3.1)$$

$$0 = \langle v_1(\cdot,t) - \hat{v}_1, \hat{v}_{1,\xi}\rangle, \qquad 0 = \langle v_2(\cdot,t) - \hat{v}_2, \hat{v}_{2,\xi}\rangle,$$

$$g_{1,t} = \mu_1(t), \qquad g_{2,t} = \mu_2(t),$$

with initial conditions (2.12),(2.13) that will be specified below.

To solve (3.1) numerically we restrict to a finite interval $[-L, L]$ and impose Dirichlet or Neumann boundary conditions. Then we use the finite element package Comsol Multiphysics^{TM}[5] with second order elements in space and a BDF method in time. As a bump function we first set $\varphi(x) = \exp(-x^2/\alpha)$ with suitable α. Later we see that the computations prove to be quite robust w.r.t. to the choice of φ.

Whenever the nonlocal terms in the nonlinearity f have to be evaluated at arguments outside the computational domain we extrapolate with the boundary values

$v_j(\pm L)$. Inside $[-L, L]$ we use linear interpolation. As in the case of freezing single waves we cannot expect the solutions $v_j(\cdot, t)$ to converge to $\hat{w}_j$ from (3.1) but rather to an approximation $\hat{w}_j^L$ that solves the stationary boundary value problem on $[-L, L]$.

3.1. Nagumo equation. A simple example is the scalar Nagumo equation [7]

$$u_t = u_{xx} + u(1-u)(u-a), \quad u(x,t) \in \mathbb{R}, \ x \in \mathbb{R}, \ t > 0, \tag{3.2}$$

where $a \in (0, \frac{1}{2})$.

It has explicit traveling waves connecting the stationary points $w_1^- = w_2^+ = 0$ and $w_1^+ = w_2^- = 1$

$$
\begin{aligned}
w_1(\xi) &= \frac{1}{1 + \exp(\frac{-\xi}{\sqrt{2}})}, \quad c_1 = \sqrt{2}\,(a - \tfrac{1}{2}), \\
w_2(\xi) &= \frac{1}{1 + \exp(\frac{\xi}{\sqrt{2}})}, \quad c_2 = -\sqrt{2}\,(a - \tfrac{1}{2}).
\end{aligned}
\tag{3.3}
$$

In addition, there exists a multitude of other solutions which can be computed explicitly [1].

We use $a = \frac{1}{4}$, the spatial stepsize $\Delta x = 0.1$ and $\hat{v}_1 = v_1^0$, $\hat{v}_2 = v_2^0$ as template functions for the phase fixing condition. As bump function we take $\varphi(\xi) = \exp(x^2/\alpha)$, where the parameter $\alpha = 20$ is chosen such that the function is localized around the region of interest (see Figure 3.4). This setting will be used for all computations with the Nagumo equation, unless indicated otherwise.

In Figures 3.1 and 3.2 we show the result of a computation starting with initial data $v_1^0, v_2^0, g_1^0, g_2^0$ that add up to a hat function u^0 via the superposition (2.14). For the numerical solution on the finite interval $[-L, L], L = 50$ we use Dirichlet boundary conditions

$$v_1(-L, t) = w_1^- = 0, \ v_2(-L, t) = 0, \ v_1(L, t) = w_1^+ = 1, \ v_2(L, t) = w_2^+ - w_2^- = -1.$$

Figure 3.1 displays the sum (1.4)

$$u_c(x,t) = v_1(x - \gamma_1(t), t) + v_2(x - \gamma_2(t), t) \tag{3.4}$$

while Figure 3.2 shows the components v_1 and v_2. The darker shaded regions indicate
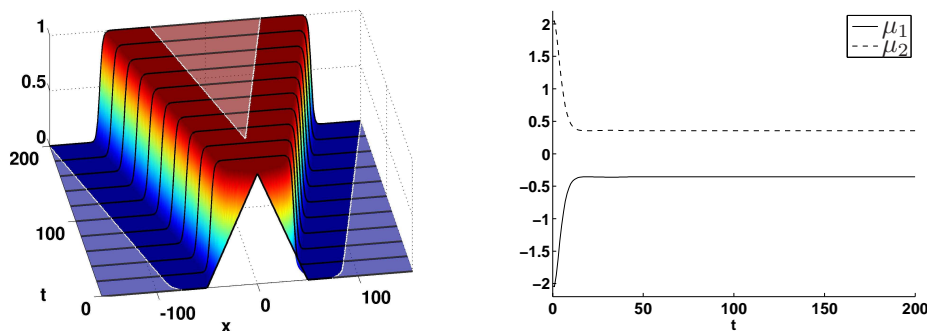

FIG. 3.1. *Fronts moving in opposite directions in the Nagumo equation, evolution of superposition u_c and velocities μ_1, μ_2.*
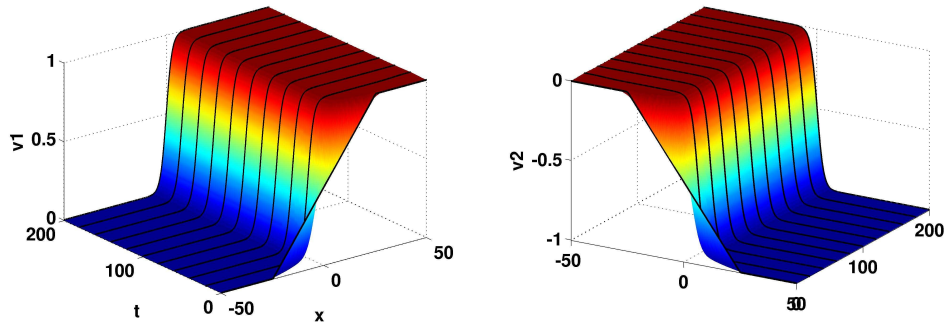
FIG. 3.2. *Fronts moving in opposite directions in the Nagumo equation, evolution of frozen fronts v_1, v_2.*

the two moving intervals $\gamma_j(t) + [-L, L], j = 1, 2$ where u_c uses the computed values of v_1 or v_2, whereas the lighter shaded regions use exclusively the extrapolated boundary values of v_1 and v_2. After a short transient period the components v_1, v_2 and the velocities μ_1, μ_2 become stationary with opposite values resulting in a broadening plateau for u. The slopes of the plateau travel at speeds $\mu_1 = -\mu_2$ in opposite directions.
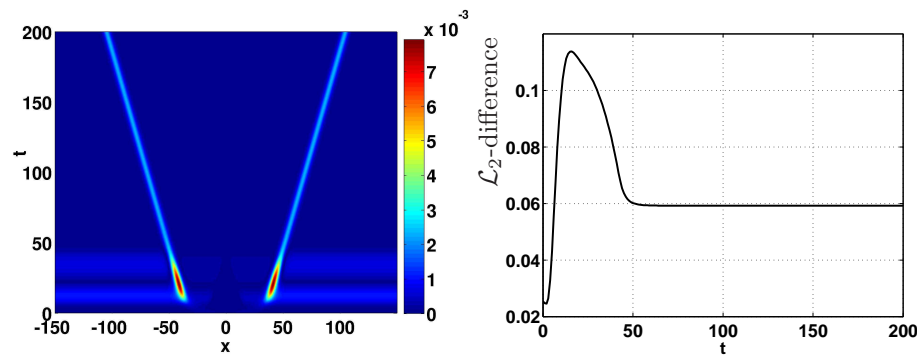
FIG. 3.3. *Nagumo equation: difference of traveling plateau and superposition of frozen fronts.*

For comparison we show in Figure 3.3 the pointwise difference $|u_{\mathrm{trav}}(x, t) - u_c(x, t)|$ and the $\mathcal{L}_2$ difference $\|u_{\mathrm{trav}}(\cdot, t) - u_c(\cdot, t)\|_{\mathcal{L}_2}$ between the function u_c and a solution u_{trav} that is obtained by solving (3.2) directly on a sufficiently large interval.

There is very good agreement of the two solutions except in two thin layers close to the two fronts. This results from a phase shift error in the superposition that can not be corrected by a single phase shift and which grows linearly for increasing t. For the individual solutions v_j of (3.1) we expect in suitable norms

$$v_j(\cdot, t) - \hat{w}_j(\cdot - \tau_j) \to 0, \quad \mu_j(t) \to c_j \quad \text{as } t \to \infty, \ j = 1, 2. \tag{3.5}$$

Since we do not use the given profiles (3.3) for the phase condition we can only expect convergence towards $\hat{w}_j(\cdot - \tau_j)$, for some suitable time shift τ_j. This shift is determined by the phase condition in (3.1), i.e. $\langle \hat{w}_j(\cdot - \tau_j) - \hat{v}_j, \hat{v}_{j,\xi} \rangle = 0$. From the last equation

in (3.5) we then obtain

$$g_j(t) - (c_j t + g_j^0) \to \tau_j \quad \text{as } t \to \infty.$$

Therefore, our numerical calculation suggests that the exact solution u_{trav} of (3.2) satisfies in a suitable norm

$$u_{\text{trav}}(\cdot, t) - \left(\hat{w}_1(\cdot - c_1 t - g_1^0 - \tau_1) + \hat{w}_2(\cdot - c_2 t - g_2^0 - \tau_2) \right) \to 0 \quad \text{as } t \to \infty$$

provided the difference of initial positions $g_2^0 - g_1^0$ is sufficiently large and the difference of initial values $u_{\text{trav}}(\cdot, 0) - \left(\hat{w}_1(\cdot - g_1^0) + \hat{w}_2(\cdot - g_2^0) \right)$ is sufficiently small. A proof of such a result is work in progress.

In Figure 3.5 we show the behavior of time derivatives $\|u_t\|$ and $\|\mu_t\|$ (left) including a comparison of $\|u_t\|$ for different bump functions (right). The second function is $\varphi(\xi) = \text{sech}(x/\beta)$, where β is chosen such that the integrals of both functions over $\mathbb{R}$ coincide, see Figure 3.4. For a certain time interval the rate of decay is the same for both bump functions. From the numerical data one finds the slope 0.25 which coincides with the spectral gap between zero and the smallest negative eigenvalue of the linearization about the single travelling waves w_1 and w_2 . This relation was verified in [20],[19] for the case of freezing a single wave. For larger times t the decay is better for the Gaussian $\varphi(x) = \exp(-x^2/\alpha)$ than for the sech-function. The effect vanishes on larger computational domains where both functions are sufficiently localized.
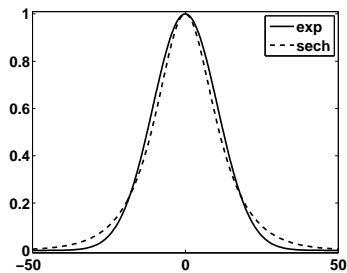

FIG. 3.4. *Comparison of functions $\varphi(x) = \exp(-x^2/\alpha)$ and $\varphi(x) = \text{sech}(-x/\beta)$ with equal integral*
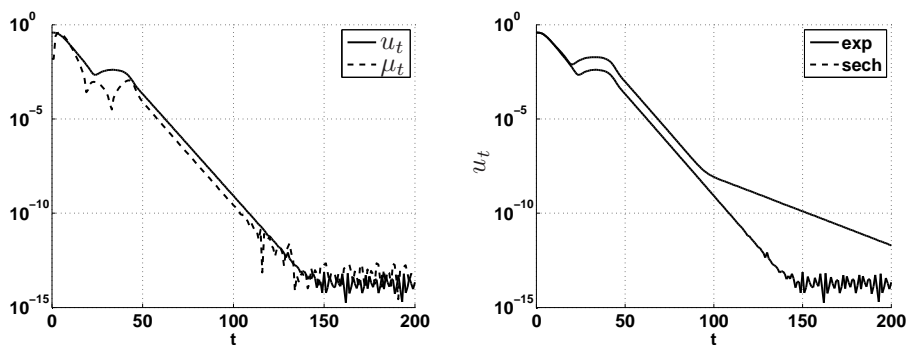

FIG. 3.5. *Nagumo equation: $\|u_t\|$ and $\|\mu_t\|$ vs. time and $\|u_t\|$ for functions $\varphi(x) = \exp(-x^2/\alpha)$ and $\varphi(x) = \text{sech}(-x/\beta)$, $\beta = 8.5$.*
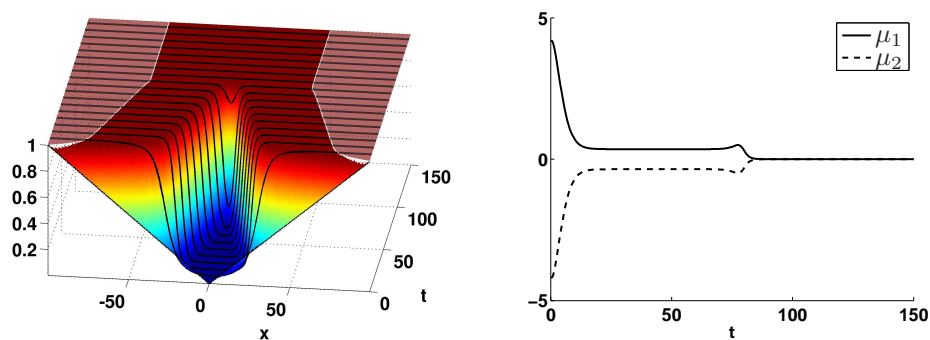
FIG. 3.6. *Collision in the Nagumo equation, evolution of superposition u_c and velocities μ_1, μ_2*
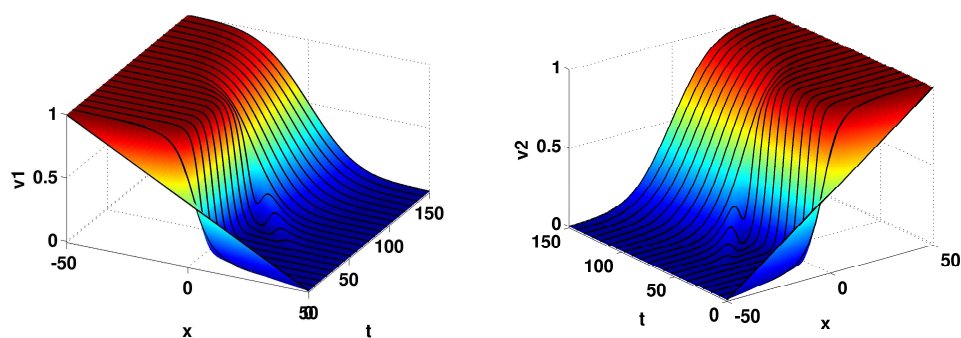

FIG. 3.7. *Collision in the Nagumo equation, evolution of frozen fronts v_1, v_2.*

In the second numerical experiment we consider a situation that, in a sense, is opposite to the first case, see Figures 3.6 and 3.7. We start with a downward hat function and obtain two fronts traveling towards each other with opposite speeds. Eventually they annihilate each other resulting in a value of zero for the speeds μ_1, μ_2. In Figure 3.7 one can observe slight disturbances in v_1, v_2 during the strong interaction at collision. Note that after the collision the superposition (1.4) yields a constant
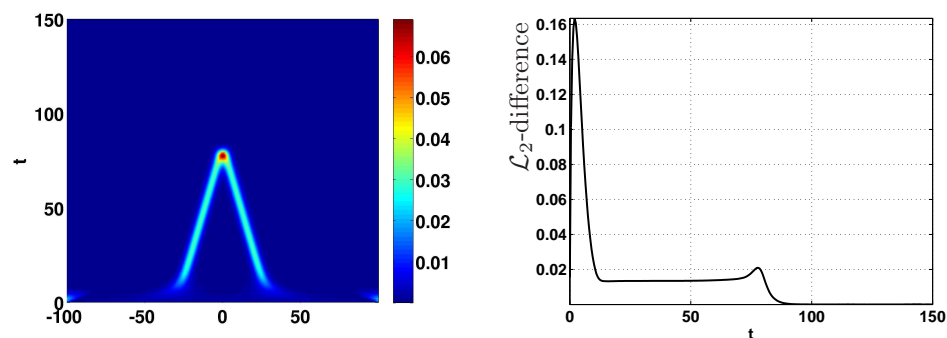

FIG. 3.8. *Collision in the Nagumo equation, evolution of difference $|u_{\text{trav}}(x,t) - u_c(x,t)|$ and of $\mathcal{L}_2$ difference $\|u_{\text{trav}}(\cdot,t) - u_c(\cdot,t)\|_{\mathcal{L}_2}$.*

although the components v_1, v_2 cannot become constant due to Dirichlet boundary conditions. Rather the asymptotic state of our system is formed by two ramp functions that are at rest and add up to a constant, see Figure 3.7. As before we observe a phase shift difference when comparing with the solution of (3.2) on a large interval, see Figure 3.8. But in this case the difference converges to zero as the constant solution is approached. Similar results are obtained for Neumann boundary conditions.

In Figures 3.9 and 3.10 we consider a case where a two-front turns into a single front. This is a case where the number N of components in our ansatz is larger than the number of components which constitute the final solution. This does not create any problems for our method. We use boundary conditions that do not require
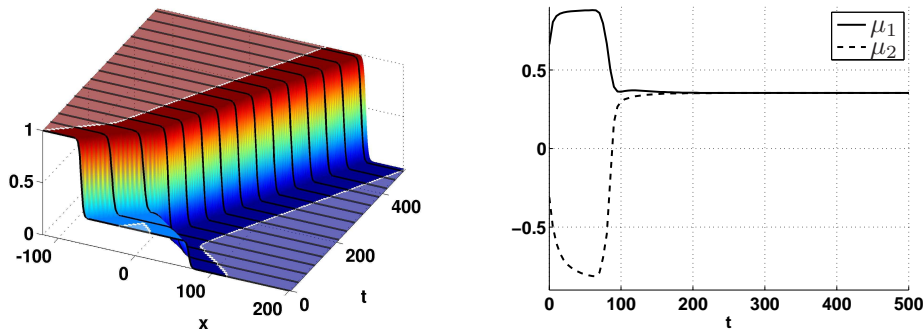

FIG. 3.9. *Merging fronts in the Nagumo equation, evolution of superposition u_c and velocities μ_1, μ_2.*
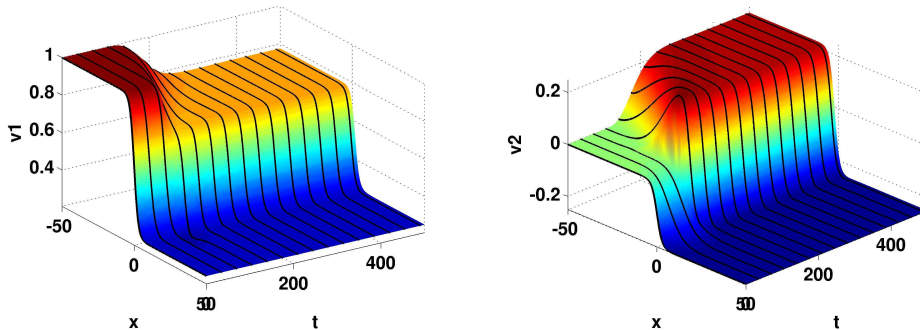

FIG. 3.10. *Merging fronts in the Nagumo equation, evolution of frozen fronts v_1, v_2.*

any a-priori knowledge of the limiting stationary points for the components v_1 and v_2. Instead of prescribing $v_1^{\pm}$ and $v_2^{\pm}$ directly, we require $v_1^- + v_2^- = w^-$ and $v_1^+ + v_2^+ = w^+$ and impose Neumann boundary conditions at the remaining ends. If one insists on Dirichlet boundary conditions for every single wave then additional boundary layers will develop.

In the current example the wave behind has a larger speed and merges with the first wave. This is correctly reproduced by our method. The speeds μ_1, μ_2 of both components converge to the same value and the superposition of the profiles v_1, v_2 forms a single front, see Figure 3.9.

In Figure 3.11 we show the difference between superposition and solution of the original equation on a large interval. After the strong interaction the rates of decay for $\|u_t\|_{\mathcal{L}_2}$ and $\|\mu_t\|$ (not shown) turn out to be quite similar to the previous case in Figure 3.5 .
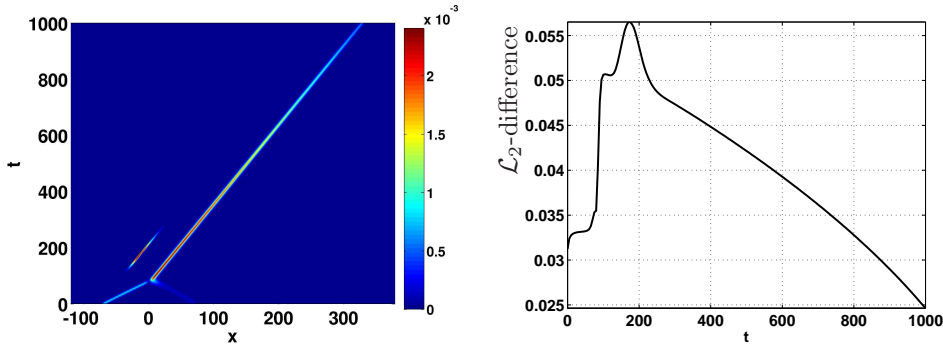

FIG. 3.11. *Nagumo, evolution of difference* $\|u_{\mathrm{trav}}(\cdot,t) - u_c(\cdot,t)\|_{\mathcal{L}_2}$

3.2. FitzHugh-Nagumo system. The two component FitzHugh-Nagumo system (FHN for short)

$$
\begin{aligned}
V_t &= V_{xx} + V - \frac{1}{3}V^3 - R, \\
R_t &= \epsilon(V + a - bR)
\end{aligned}
\tag{3.6}
$$

models nerve conduction and possesses different types of traveling wave solutions such as fronts, multifronts [11] and pulses [9], [10]. We consider the same parameters $a = 0.7, b = 0.8, \epsilon = 0.08$ as in [3] for which traveling pulses exist. Because of reflectional symmetry, with each solution its mirror image is also a solution traveling at opposite speed. It is important to note that, due to the lack of diffusion in the second equation of (3.6), the PDAE system (3.1) is of mixed hyperbolic-parabolic type. In the two R-equations the convective terms that allow freezing, form the principal part and this requires some cautionary measure for the numerical solution. With the finite element code Comsol Multiphysics$^{\mathrm{TM}}$ we used streamline diffusion ($\delta_{sd} = 0.25$)
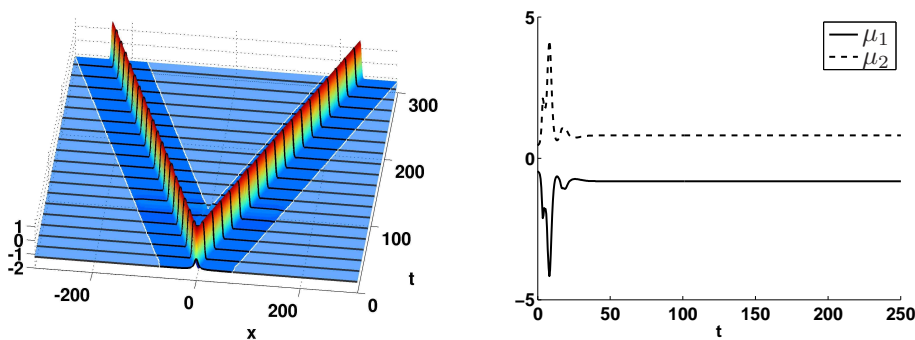

FIG. 3.12. *Splitting of a pulse in the FHN system, evolution of superposition* $V = u_c$ *and of velocities* μ_1, μ_2.
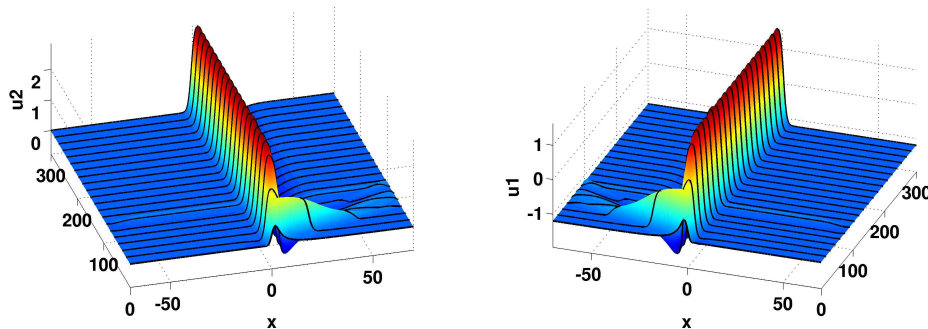
FIG. 3.13. *Splitting of a pulse in the FHN system, evolution of pulses V_1 traveling to the left and V_2 traveling to the right.*

in order to treat the hyperbolic part correctly. The system is solved on $[-70, 70]$ with Dirichlet boundary conditions, stepsize $\Delta x = 0.1$ and $\varphi(x) = \operatorname{sech}(x/\beta)$, $\beta = 11.3$ (results for a Gaussian φ are similar).

First we consider the formation of two pulses out of a single initial pulse. This situation was already studied in [3] with the single freezing method. There only one of the two forming pulses could be frozen depending on the choice of phase condition. Figure 3.12 displays the behavior of the superposition (1.4) as obtained by our method and Figure 3.14 shows the difference to a solution of (3.6) obtained directly on a large interval. The difference is small in most of the space time domain.

In Figure 3.13 one observes that the components V_1 and V_2 develop tiny secondary waves that travel towards the boundary. The superposition is still correct until these reach the boundary. When they arrive a slight disturbance of the superposition in the middle of the interval develops (at about $t = 90$, see Figure 3.14). We expect that these boundary effects can be further reduced by using e.g. transparent boundary conditions. After the separation phase both pulses quickly reach their asymptotic states, see Figure 3.13, and $||u_t||$ decays exponentially as in the Nagumo case, see Figure 3.15.
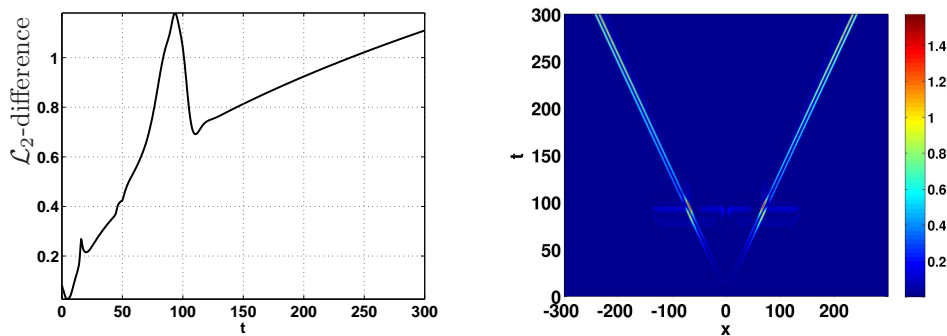

FIG. 3.14. *Splitting of a pulse in the FHN system, difference of the two-pulse computed on a large domain and superposition of frozen single pulses V_1, V_2.*

Now we take the two traveling pulses which have been computed in this way and interchange their initial positions g_j^0. Then the two pulses start to move towards
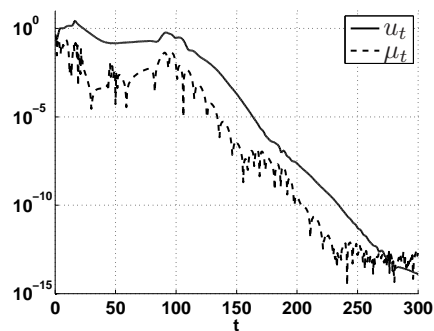
Fig. 3.15. *Splitting of a pulse in the FHN system, time behavior of $\|u_t\|, u = (V_1, R_1, V_2, R_2)$ and $\|\mu_t\|$.*

each other and eventually annihilate as shown in Figure 3.16. The difference of the superposition and the solution of the original equation on a large domain behaves in quite a similar fashion as in the Nagumo case. At the collision both wave speeds converge to zero. Figure 3.17 shows that both components V_1 and V_2 converge to constants.
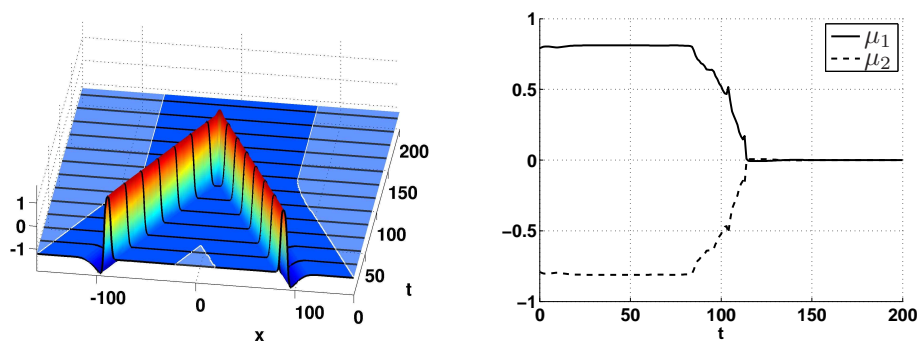

Fig. 3.16. *Collision of pulses in the FHN system, evolution of superposition $u_c = V$ and velocities μ_1, μ_2.*
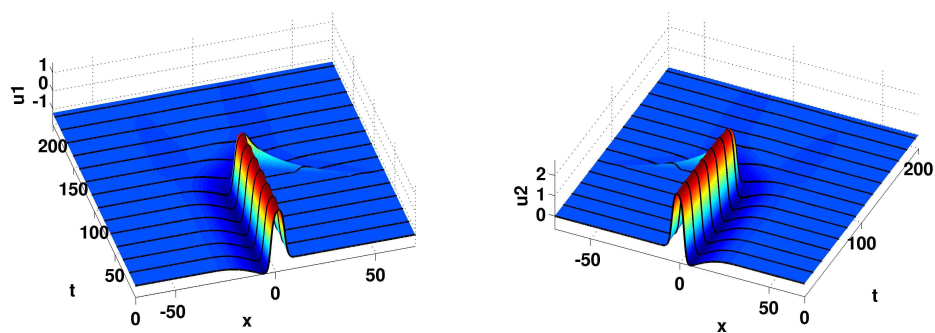

Fig. 3.17. *Collision of pulses in the FHN system, evolution of frozen pules V_1, V_2.*

Contrary to the case of fronts this can lead to numerical difficulties for large times since our phase conditions ar no longer well posed for constant functions (cf. (2.16), (2.17)). We note that after collision we have again the situation, where we use a larger number N than necessary for representing the solution and where our method reproduces the behavior in a consistent manner.

4. Asymptotic properties of multifronts. In this section we show that traveling waves, when shifted as in (2.2), satisfy the PDAE system (2.8) in an asymptotic sense as $t \to \infty$. This will imply a corresponding property of the superposition (2.2) for the original system (1.1).

DEFINITION 4.1. *A smooth function $V : \mathbb{R}^N \to \mathbb{R}^m$ is called an **asymptotic N-front solution** of (1.1) if there exist constants*

$$c_1, c_2, \ldots, c_N$$

such that

$$u(x,t) = V(x - c_1 t, \ldots, x - c_N t) \tag{4.1}$$

satisfies

$$\|(u_t - A u_{xx} - f(u, u_x))(\cdot, t)\|_{\mathcal{L}_2} \to 0 \quad as \ t \to \infty. \tag{4.2}$$

We look for asymptotic N-front solutions of the type

$$V(x_1, \ldots, x_N) = \sum_{j=1}^{N} \hat{w}_j(x_j) \tag{4.3}$$

where $\hat{w}_j$ is defined in (2.2) and $w_j(x - c_j t)$ are C^2-smooth traveling waves of (1.1). In particular, they satisfy the stationary equation

$$0 = A w_{j,\xi\xi} + c_j w_{j,\xi} + f(w_j, w_{j,\xi}). \tag{4.4}$$

With (2.10) let us write (2.8) as

$$v_{j,t} = M_j(v,g) = A v_{j,\xi\xi} + v_{j,\xi} g_{j,t} + F_j(v,g), \quad j = 1, \ldots, N. \tag{4.5}$$

For the special functions

$$v_j = \hat{w}_j, \ g_j(t) = c_j t, j = 1, \ldots, N, t \in \mathbb{R}_+, \tag{4.6}$$

we show in Theorem 4.2 below

$$\|M_j(\hat{w}, g)(\cdot, t)\|_{\mathcal{L}_2} \to 0 \quad \text{as } t \to \infty, \tag{4.7}$$

i.e. they are asymptotic steady states of the nonautonomous system (4.5). Using the basic calculation (2.6) we obtain that

$$u(x,t) = \sum_{j=1}^{N} \hat{w}_j(x - c_j t) \tag{4.8}$$

satisfies the estimate

$$||(u_t - Au_{xx} - f(u, u_x))(\cdot, t)||_{\mathcal{L}_2}$$
$$= ||\sum_{j=1}^{N} M_j(\hat{w}, g)(\cdot - c_j t, t)||_{\mathcal{L}_2} \to 0 \quad \text{as } t \to \infty.$$

Therefore, the function (4.3) is an asymptotic N-front solution.

THEOREM 4.2. *Let $w_j(x - c_j t), j = 1, \ldots, N$ be C^2 smooth traveling wave solutions of the system (1.1) that satisfy for some constants $C, \alpha > 0$*

$$c_1 < c_2 < \ldots < c_N, \tag{4.9}$$

$$\|w_j(\xi) - w_j^{\pm}\| \le C e^{\mp \alpha \xi} \quad and \quad \|w_{j,\xi}(\xi)\| \le C e^{-\alpha|\xi|} \quad j = 1, \ldots, N, \tag{4.10}$$

$$w_j^+ = w_{j+1}^-, \quad j = 1, \ldots, N - 1. \tag{4.11}$$

Moreover, let $\varphi \in C^{\infty}(\mathbb{R}, \mathbb{R})$ be a function for which the exponential estimate

$$C_0 e^{-\beta_0 |x|} \le \varphi(x) \le C_1 e^{-\beta_1 |x|}, \quad x \in \mathbb{R} \tag{4.12}$$

holds for some positive constants $C_0 \le C_1$ and $\beta_1 < \beta_0$.
Then the shifted waves $\hat{w}_j$ from (2.2) and $g_j(t) = c_j t$ satisfy for some constants $C, \varepsilon > 0$

$$||M_j(\hat{w}, g)(\cdot, t)||_{\mathcal{L}_2} \le C e^{-\varepsilon t} \quad \forall t \ge 0, \tag{4.13}$$

where M_j denotes the right hand side in the PDAE system (4.5). In particular, $V(x_1, \ldots, x_N) = \sum_{j=1}^{N} \hat{w}_j(x_j)$ is an asymptotic N-front solution of equation (1.1).

REMARK 4.3. *Clearly, this result does not yet prove the behavior of the numerical solutions observed in Section 3. For such a result we must show that the PDAE system (4.5) is well-posed and, moreover, that for stable traveling waves the solutions $v_j(\cdot, t)$ converges to $\hat{w}_j$ in a suitable way as $t \to \infty$ for sufficiently small initial perturbations. We think of Theorem 4.2 being a first step towards such a result that justifies the overall ansatz in Section 2.*

REMARK 4.4. *The theorem remains valid for more general bump functions that satisfy*

$$C_0 e^{-\beta_0 |x|^k} \le \varphi(x) \le C_1 e^{-\beta_1 |x|^k}, \quad x \in \mathbb{R} \quad with \ 0 < C_0 \le C_1, 0 < \beta_1 < \beta_0, k \ge 1.$$

The case $k = 2$ was used in some of our simulations above. The following proof will show that the only modifications occur in the estimates on the intervals marked by Q_j^g in Figure 4.1 and in the condition (4.17) that determines the subdivision of the real line.

Proof. Let us first note that (4.10) and (4.4) imply $\lim_{\xi \to \pm \infty} w_{j,\xi\xi}(\xi) = 0$ and hence

$$f(w_j^{\pm}, 0) = 0. \tag{4.14}$$

As noted above it suffices to prove (4.13). For the ease of reading we restrict to the case where f depends on u only, $f(u, u_x) = f(u)$. Using (4.14), (4.4) and (4.10) the

details of the general case can be filled in easily. In the following we use C to denote a generic constant. First, the stationary equation (4.4) yields

$$
\begin{aligned}
||M_j(\hat{w},g)(\cdot,t)||^2_{\mathcal{L}_2} =&||Q^g_j(\cdot,t)f(\sum_{k=1}^{N}\hat{w}_k(\xi^g_{k,j})) - f(w_j)||^2_{\mathcal{L}_2} \\
\leq& C\left[\int_{\mathbb{R}} Q^g_j(\xi,t)^2|f(\sum_{k=1}^{N}\hat{w}_k(\xi^g_{k,j})) - f(w_j(\xi))|^2 d\xi \right. \\
&\left. + \int_{\mathbb{R}}(1 - Q^g_j(\xi,t))^2|f(w_j(\xi))|^2 d\xi \right] =: I_1 + I_2.
\end{aligned}
$$

We estimate the integrals I_1, I_2 separately. When comparing f arguments we frequently use the following equality

$$
\sum_{k=1}^{N}\hat{w}_k(\xi^g_{kj}) - w_j(\xi) = \sum_{k=1}^{j-1}(w_k(\xi^g_{kj}) - w^+_k) + \sum_{k=j+1}^{N}(w_k(\xi^g_{kj}) - w^-_k). \tag{4.15}
$$

Consider first I_1 and indices $2 \leq j \leq N - 1$. For $q > 0$ sufficiently small we define

$$
\gamma^{\pm}_k = (1 \pm q)(c_k - c_j)t, \qquad \gamma^0_k = (c_k - c_j)t
$$

and partition $\mathbb{R}$ into subintervals as follows (cf. Figure 4.1)

$$
\begin{aligned}
-\infty < \gamma^+_1 < \gamma^0_1 < \gamma^-_1 < \gamma^+_2 < \ldots < \gamma^+_{j-1} < \gamma^0_{j-1} < \gamma^-_{j-1} < 0 = \gamma^{\pm}_0 \\
< \gamma^-_{j+1} < \gamma^0_{j+1} < \gamma^+_{j+1} < \ldots < \gamma^-_N < \gamma^0_N < \gamma^+_N < \infty. \tag{4.16}
\end{aligned}
$$

Note that the relations $\gamma^-_k < \gamma^+_{k+1}$ for $k \leq j-1$ and $\gamma^+_k < \gamma^-_{k+1}$ for $k \geq j+1$ follow if q satisfies

$$
q < \min\left\{\frac{c_{k+1} - c_k}{|2c_j - c_k - c_{k+1}|} \;:\; 1 \leq j \leq N,\; 1 \leq k \leq N-1\right\}.
$$
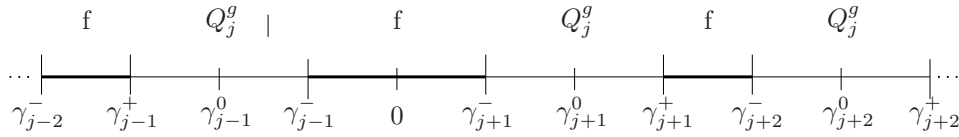
FIG. 4.1. *Decomposition of the interval $\mathbb{R}$.*

Our second condition on q is

$$
q < \frac{\min\left(\min\limits_{j=2,\ldots,N}(c_j - c_{j-1}), 1\right)\beta_1}{\max\left(\max\limits_{j=2,\ldots,N}(c_j - c_{j-1}), 1\right)(\beta_1 + \beta_0)}. \tag{4.17}
$$

For the estimate of I_1 we use $0 \leq Q^g_j(\cdot,\cdot) \leq 1$ and the fact that all arguments of f lie in a compact interval. On each subinterval we use either the smallness of f or of Q^g_j

as indicated in Figure 4.1. We obtain

$$
\begin{aligned}
I_1 \leq C &\left[\int_{-\infty}^{\gamma_1^+} |f(\sum_{k=1}^{N} \hat{w}_k(\xi_{k,j}^g)) - f(w_j(\xi))|^2 d\xi + \sum_{l=1}^{j-1} \int_{\gamma_l^+}^{\gamma_l^0} Q_j^g(\xi,t)^2 d\xi \right. \\
&+ \sum_{l=1}^{j-1} \int_{\gamma_l^0}^{\gamma_l^-} Q_j^g(\xi,t)^2 d\xi + \sum_{l=1}^{j-2} \int_{\gamma_l^-}^{\gamma_{l+1}^+} |f(\sum_{k=1}^{N} \hat{w}_k(\xi_{k,j}^g)) - f(w_j(\xi))|^2 d\xi \\
&+ \int_{\gamma_{j-1}^-}^{\gamma_{j+1}^-} |f(\sum_{k=1}^{N} \hat{w}_k(\xi_{k,j}^g)) - f(w_j(\xi))|^2 d\xi + \sum_{l=j+1}^{N} \int_{\gamma_l^-}^{\gamma_l^0} Q_j^g(\xi,t)^2 d\xi \\
&+ \sum_{l=j+1}^{N} \int_{\gamma_l^0}^{\gamma_l^+} Q_j^g(\xi,t)^2 d\xi + \sum_{l=j+1}^{N-1} \int_{\gamma_l^+}^{\gamma_{l+1}^-} |f(\sum_{k=1}^{N} \hat{w}_k(\xi_{k,j}^g)) - f(w_j(\xi))|^2 d\xi \\
&\left. + \int_{\gamma_N^+}^{\infty} |f(\sum_{k=1}^{N} \hat{w}_k(\xi_{k,j}^g)) - f(w_j(\xi))|^2 d\xi \right] \\
=: & I_1^b + \sum_{l=1}^{j-1} I_{1,l}^{1-} + \sum_{l=1}^{j-1} I_{1,l}^{2-} + \sum_{l=1}^{j-2} I_{1,l}^{3-} + I_1^c \\
&+ \sum_{l=j+1}^{N} I_{1,l}^{1+} + \sum_{l=j+1}^{N} I_{1,l}^{2+} + \sum_{l=j+1}^{N-1} I_{1,l}^{3+} + I_1^e.
\end{aligned}
$$

For the convenience of the reader we give here only the estimate for the crucial central term I_1^c and defer the remaining laborious estimates to the appendix. With (4.9), (4.10), (4.11) and (4.15) we obtain

$$
\begin{aligned}
I_1^c \leq & C \int_{\gamma_{j-1}^-}^{\gamma_{j+1}^-} |\sum_{k=1}^{N} \hat{w}_k(\xi + (c_j - c_k)t) - w_j(\xi)|^2 d\xi \\
\leq & C \int_{\gamma_{j-1}^-}^{\gamma_{j+1}^-} \left(\sum_{k=1}^{j-1} |w_k(\xi + (c_j - c_k)t) - w_k^+|^2 + \sum_{k=j+1}^{N} |w_k(\xi + (c_j - c_k)t) - w_k^-|^2 \right) d\xi \\
\leq & C \left[\int_{\gamma_{j-1}^-}^{\gamma_{j+1}^-} \sum_{k=1}^{j-1} e^{-2\alpha(\xi + (c_j - c_k)t)} d\xi + \int_{\gamma_{j-1}^-}^{\gamma_{j+1}^-} \sum_{k=j+1}^{N} e^{2\alpha(\xi + (c_j - c_k)t)} d\xi \right] \\
\leq & C \left[\int_{\gamma_{j-1}^-}^{\gamma_{j+1}^-} e^{-2\alpha(\xi + (c_j - c_{j-1})t)} d\xi + \int_{\gamma_{j-1}^-}^{\gamma_{j+1}^-} e^{2\alpha(\xi + (c_j - c_{j+1})t)} d\xi \right] \\
\leq & C \left[e^{-2\alpha q(c_j - c_{j-1})t} + e^{-2\alpha q(c_{j+1} - c_j)t} \right].
\end{aligned}
$$

□

5. Generalization to equivariant evolution equations. In this section we generalize the idea from Section 2 to evolution equations in Banach spaces that are equivariant with respect to the action of a Lie group. The abstract setting follows the approach from [3],[4].

5.1. The abstract formulation. Consider an evolution equation

$$
u_t = Au + F(u), \quad u(0) = u_0 \tag{5.1}
$$

where $A, F : Y \subset X \to X$ are linear resp. nonlinear operators from a dense subspace Y of some Banach space X into X. We assume equivariance of both A and F with respect to some action of the Lie group G on X

$$a : G \to GL(X), \ g \mapsto a(g),$$

that is

$$F(a(g)u) = a(g)F(u), \quad A(a(g)u) = a(g)Au \qquad (5.2)$$

holds for all $u \in Y$, $g \in G$. In order to mimic the partition of unity construction we assume that there is a module E (i.e. a real vector space with an Abelian multiplication) acting on X via

$$\bullet : E \times X \to X, \ (\varphi, u) \mapsto \varphi \cdot u,$$

such that both distributive laws and the associative law hold.

Moreover, we assume that the group also acts on E via a possibly different action

$$\alpha : G \to GL(E), \ g \mapsto \alpha(g),$$

such that for all $g \in G$, $\varphi, \psi \in E$, $u \in X$

$$\alpha(g)(\varphi\psi) = (\alpha(g)\varphi)(\alpha(g)\psi) \qquad (5.3)$$
$$a(g)(\varphi \cdot u) = (\alpha(g)\varphi) \cdot (a(g)u). \qquad (5.4)$$

Furthermore, we assume that the map

$$a(\cdot)u : G \to X, \quad g \mapsto a(g)u$$

is continuous for any $u \in X$ and that it is continuously differentiable for any $u \in Y$ with derivative denoted by

$$d[a(g)u] : T_g G \to X, \quad \lambda \mapsto d[a(g)u]\lambda.$$

EXAMPLE 5.1. *Consider as an example $X = \mathcal{L}^2(\mathbb{R}, \mathbb{C})$, $G = S^1 \times \mathbb{R}$ with the action given by*

$$[a(\theta, \tau)u](x) = e^{i\theta}u(x - \tau), \quad u \in X, \ (\theta, \tau) \in S^1 \times \mathbb{R}. \qquad (5.5)$$

Then with $E = C_{unif}^0(\mathbb{R}, \mathbb{R})$ we find that (5.3),(5.4) hold for the setting $\alpha(\theta, \tau)\varphi(x) = \varphi(x - \tau)$ for $\varphi \in E$. Moreover, with this choice the action is continuous on E. We note, however, that this property will not be needed for the arguments to follow.

In the following we assume that we are given some $\varphi \in E$ such that $\sum_{j=1}^N \alpha(g_j)\varphi$ is invertible for any choice of $g_j \in G$. In Section 2 and in Example 5.1 above this property is a consequence of (2.5). For the inverse element of some $\varphi \in E$ we use the notation $\frac{1}{\varphi} = \varphi^{-1}$.

The generalization of (1.4) is to write the solution u as

$$u(t) = \sum_{j=1}^N a(g_j(t))v_j(t), \qquad (5.6)$$

with unknowns $g_j(t) \in G$, $v_j \in Y$. Inserting into (5.1) and using equivariance (5.2) as well as (5.3),(5.4) leads to

$$
\begin{aligned}
u_t &= \sum_{j=1}^{N} \left(a(g_j)v_{j,t} + d[a(g_j)v_j]g_{j,t} \right) \\
&= \sum_{j=1}^{N} A(a(g_j)v_j) + F\left(\sum_{k=1}^{N} a(g_k)v_k \right) \\
&= \sum_{j=1}^{N} a(g_j)Av_j + \sum_{j=1}^{N} \frac{\alpha(g_j)\varphi}{\sum_{k=1}^{N} \alpha(g_k)\varphi} \cdot F\left(\sum_{k=1}^{N} a(g_k)v_k \right) \\
&= \sum_{j=1}^{N} a(g_j) \left[Av_j + \frac{\varphi}{\sum_{k=1}^{N} \alpha(g_j^{-1}g_k)\varphi} \cdot F\left(\sum_{k=1}^{N} a(g_j^{-1}g_k)v_k \right) \right].
\end{aligned}
$$

This equation is fulfilled if the v_j, g_j satisfy the following system

$$
v_{j,t} = Av_j + \frac{\varphi}{\sum_{k=1}^{N} \alpha(g_j^{-1}g_k)\varphi} \cdot F\left(\sum_{k=1}^{N} a(g_j^{-1}g_k)v_k \right) - a(g_j^{-1})d[a(g_j)v_j]g_{j,t}. \quad (5.7)
$$

We simplify the last term as in [4]. Let $\mathbb{1}$ be the unit element in G, then the tangent space $T_{\mathbb{1}}G$ is the Lie algebra associated with G. By $dg(\mathbb{1}) : T_{\mathbb{1}}G \to T_g G$ we denote the derivative of the multiplication from the left by g at $\mathbb{1}$. Differentiating the relation $a(g \circ \gamma)v = a(g)(a(\gamma)v)$ for $v \in Y$ at $\gamma = \mathbb{1}$ yields

$$
a(g)d[a(\mathbb{1})v]\mu = d[a(g)v](dg(\mathbb{1})\mu) \quad \text{for } \mu \in T_{\mathbb{1}}G, v \in Y.
$$

Therefore, defining new coordinates $\mu_j(t) \in T_{\mathbb{1}}G$ by $g_{j,t}(t) = dg_j(\mathbb{1})\mu_j(t)$ turns equation (5.7) into

$$
\begin{aligned}
v_{j,t} &= Av_j + \frac{\varphi}{\sum_{k=1}^{N} a(g_j^{-1}g_k)\varphi} \cdot F\left(\sum_{k=1}^{N} a(g_j^{-1}g_k)v_k \right) - d[a(\mathbb{1})v_j]\mu_j, \\
&= Av_j + \mathcal{F}_j(v,g) - d[a(\mathbb{1})v_j]\mu_j
\end{aligned} \quad (5.8)
$$

and

$$
g_{j,t} = dg_j(\mathbb{1})\mu_j. \quad (5.9)
$$

As usual we add initial data

$$
v_j(0) = v_{j,0}, \ \ g_j(0) = g_{j,0} \quad j = 1, \ldots, N \quad (5.10)
$$

that should satisfy

$$
u_0 = \sum_{j=1}^{N} a(g_{j,0})v_{j,0}. \quad (5.11)
$$

Finally, we assume that a continuous inner product $\langle \cdot, \cdot \rangle_2$ on X is available and use this to derive N phase conditions each of dimension $\dim(G)$. Suppose we have template functions $\hat{v}_j$ and require the distance $\mathrm{dist}(v_j, \mathcal{O}(\hat{v}_j)) = \inf_{g \in G} \|v_j - a(g)\hat{v}_j\|_2$

to the group orbit $\mathcal{O}(\hat{v}_j) = \{a(g)v_j : g \in G\}$ to achieve its minimum at $g = \mathbb{1}$. Then we find the necessary condition

$$\langle v_j - \hat{v}_j, d[a(\mathbb{1})\hat{v}_j]\lambda\rangle_2 = 0, \quad \forall \lambda \in T_\mathbb{1}G, j = 1, \dots, N. \tag{5.12}$$

While this generalizes (2.15) the corresponding generalization of (2.17) is

$$\langle v_{j,t}, d[a(\mathbb{1})v_j]\lambda\rangle_2 = 0, \quad \forall \lambda \in T_\mathbb{1}G, j = 1, \dots, N. \tag{5.13}$$

Note that this requires $v_{j,t}$ to be orthogonal to the group orbit $\mathcal{O}(v_j)$ at all times. When $v_{j,t}$ from (5.8) is inserted into (5.13) we obtain a linear system of dimension $\dim(G)$ for $\mu_j(t) \in T_\mathbb{1}G$ that has a unique solution provided $d[a(\mathbb{1})v_j] : T_\mathbb{1}G \to X$ is one to one.

To realize the above abstract equations in $\mathbb{R}^s$, where $s = \dim G$ we take a basis $\{e^1, \dots, e^s\}$ in the Lie algebra $T_\mathbb{1}G$ and write $\mu_j = \sum_{i=1}^s \mu_{j,i}e^i$. Then the differentiated form of (5.12) and (5.13) reads (cf. (2.16), (2.17))

$$\hat{B}_j\mu_j = \hat{r}_j, \text{ where } \left((\hat{B}_j)_{ik}\right)_{i,k=1}^s = \left(\langle d[a(\mathbb{1})v_j]e^k, \ d[a(\mathbb{1})\hat{v}_j]e^i\rangle_{\mathcal{L}_2}\right)_{i,k=1}^s \in \mathbb{R}^{s,s},$$
$$\hat{r}_j = \left(\langle Av_j + \mathcal{F}_j(v,g), \ d[a(\mathbb{1})\hat{v}_j]e^i\rangle_{\mathcal{L}_2}\right)_{i=1}^s \tag{5.14}$$

and

$$B_j\mu_j = r_j, \text{ where } ((B_j)_{ik})_{i,k=1}^s = \left(\langle d[a(\mathbb{1})v_j]e^k, \ d[a(\mathbb{1})v_j]e^i\rangle_{\mathcal{L}_2}\right)_{i,k=1}^s \in \mathbb{R}^{s,s},$$
$$r_j = \left(\langle Av_j + \mathcal{F}_j(v,g), \ d[a(\mathbb{1})v_j]e^i\rangle_{\mathcal{L}_2}\right)_{i=1}^s. \tag{5.15}$$

Altogether we have to solve the differential algebraic system (5.8), (5.10) with phase conditions (5.14) or (5.15).

5.2. An application to the Ginzburg Landau equation.

The cubic quintic Ginzburg Landau equation [18],[21]

$$u_t = \alpha u_{xx} + \delta u + f(u), \quad f(u) = \beta|u|^2u + \gamma|u|^4u, \tag{5.16}$$
$$= \alpha u_{xx} + F(u)$$

with $\delta \in \mathbb{R}$, $\alpha, \beta, \gamma \in \mathbb{C}$, $u(x,t) \in \mathbb{C}$ shows a variety of coherent structures, like pulses, fronts, sources and sinks [21]. For certain parameter values this equation exhibits stable rotating pulses [18] as well as fronts that rotate and travel simultaneously. Equation (5.16) has the same equivariance as Example 5.1. Thus we write u as

$$u(x,t) = \sum_{j=1}^N e^{-i\theta_j(t)}v_j(x - \tau_j(t), t) \tag{5.17}$$

and define $\mu_j^\theta(t)$ by $\theta_{j,t}(t) = \mu_j^\theta(t)$ and $\mu_j^\tau(t)$ by $\tau_{j,t}(t) = \mu_j^\tau(t)$. The system (5.8) is of the form

$$v_{j,t}(\xi,t) = Av_j(\xi,t) + i\mu_j^\theta(t)v_j(\xi,t) + \mu_j^\tau(t)v_{j,\xi}(\xi,t)$$
$$+ \frac{\varphi(\xi)}{\sum_{k=1}^N \varphi(\xi - \tau_k(t) + \tau_j(t))} F\left(\sum_{k=1}^N e^{-i(\theta_k(t)-\theta_j(t))}v_k(\xi - \tau_k(t) + \tau_j(t), \ t)\right).$$

The phase conditions are derived from the $\mathcal{L}_2$-inner product in the corresponding two dimensional real system.

$$0 = \langle \mathrm{Re}(v_j - \hat{v}_j), \mathrm{Re}(\hat{v}_{j,\xi}) \rangle_{\mathcal{L}_2} + \langle \mathrm{Im}(v_j - \hat{v}_j), \mathrm{Im}(\hat{v}_{j,\xi}) \rangle_{\mathcal{L}_2},$$
$$0 = \langle \mathrm{Re}(v_j - \hat{v}_j), \mathrm{Im}(\hat{v}_j) \rangle_{\mathcal{L}_2} - \langle \mathrm{Im}(v_j - \hat{v}_j), \mathrm{Re}(\hat{v}_j) \rangle_{\mathcal{L}_2}, \qquad j = 1, \dots, N.$$

For numerical computations we used the parameters $a = 1$, $\delta = -0.1$, $\beta = 3 + i$, $\gamma = -2.75 + i$ for which the fronts and pulses mentioned above exist.

We first look at the case where the solution for the original system consists of two waves that rotate at the same speed but travel in opposite directions. As Figure 5.1 shows this is reproduced correctly by our method. The values obtained from extrapolation are shown in grey colors.
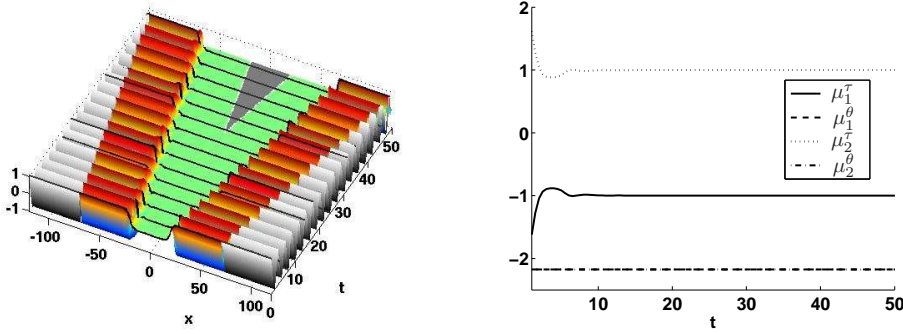

FIG. 5.1. *Fronts moving in opposite directions in the QCGL system. Evolution of superposition* $\mathrm{Re}(u_c)$ *and velocities* $\mu_1^\tau, \mu_1^\theta, \ \mu_2^\tau, \mu_2^\theta$.
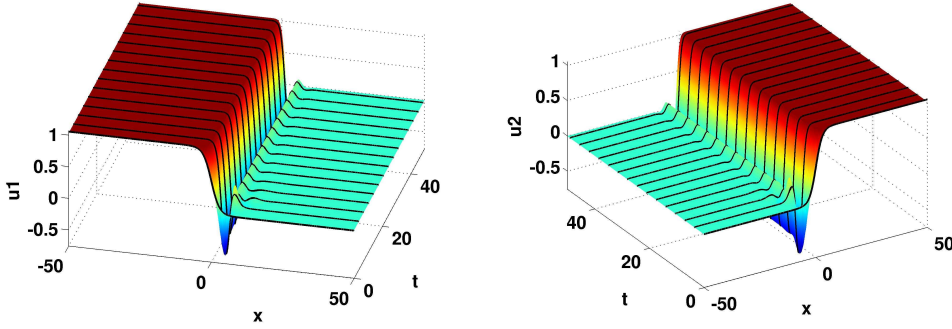

FIG. 5.2. *Fronts moving in opposite directions in the QCGL system, evolution of frozen fronts* $u_1 = \mathrm{Re}(v_1), u_2 = \mathrm{Re}(v_2)$.

The components v_1, v_2 given in Figure 5.2 become stationary and the parameters μ_i^τ, μ_i^θ, $i = 1, 2$ converge quickly to the correct values for the velocities of rotation and translation. Again the difference to a solution of the QCGL problem (5.16) on a large domain gives similar results as in Section 3.1 (not shown) and the decay of the time derivative is exponential as before, see Figure 5.3 (left). Figures 5.4 and 5.5 show another result in a case where the multipulse consists of a rotating stationary pulse and a rotating traveling front with the decay rate displayed in Figure 5.3 (right).
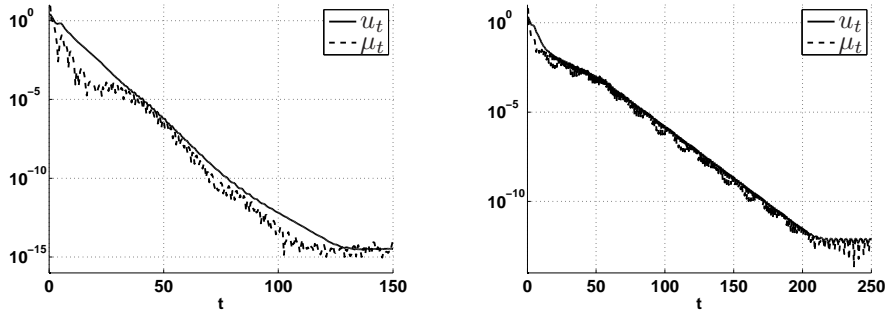
FIG. 5.3. *Fronts moving in opposite directions in the QCGL system, evolution of temporal change* $\|u_t\|_{\mathcal{L}_2}$ *and* $\|\mu_t\|$ *for two fronts (left) and pulse and front (right).*
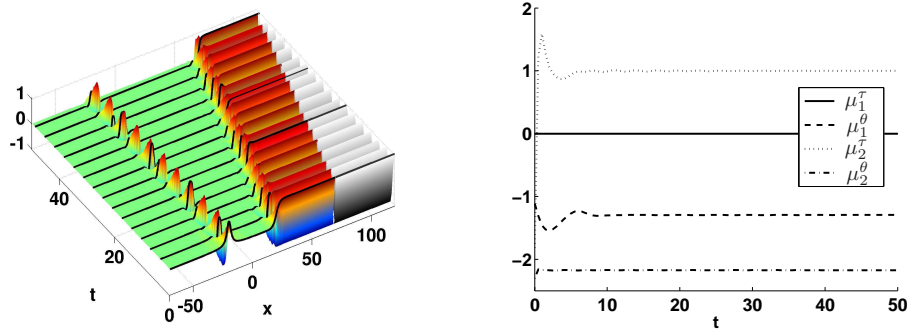

FIG. 5.4. *Pulse and front moving in opposite directions in the QCGL system, evolution of superposition* $\mathrm{Re}(u_c)$ *and velocities* $\mu_1^\tau, \mu_1^\theta, \ \mu_2^\tau, \mu_2^\theta.$
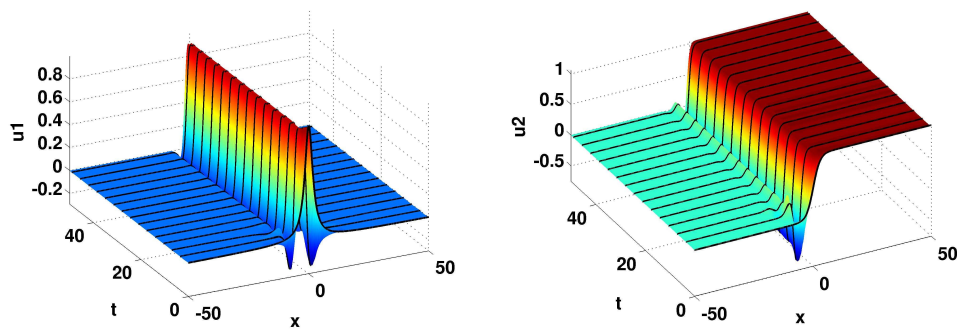

FIG. 5.5. *Pulse and front moving in opposite directions in the QCGL system, evolution of frozen pulse* $u_1 = \mathrm{Re}(v_1)$ *and front* $u_2 = \mathrm{Re}(v_2)$.

6. Conclusions. We propose a numerical method for separating drifting motions of interacting pulses and fronts in a nonlinear reaction diffusion system. The method builds on an earlier approach for freezing single pulses and fronts in a co-moving frame that is determined by the numerical process. The contribution of this paper is to embed the given equation into a system of N PDEs where N is at least the number of pulses resp. fronts that is expected for the solution. An essential feature of the approach is to decompose the nonlinear vector field by a time-dependent partition of unity into local parts that decouple when pulses and fronts are far apart. Each subsystem is expected to describe a single front or pulse in its own moving reference frame, and the superposition of these single solutions provides an exact solution of the original system. Except for the nonlinear coupling terms each subsystem retains a certain shift symmetry that is made use of by imposing appropriate phase conditions. Altogether, a system of partial differential algebraic equations (PDAEs) arises that is solved numerically by restricting to a finite domain and employing suitable time integrators.

There are at least two advantages of our method over solving the original equation on a - potentially very large - domain. Each subsystem can be solved on a relatively small and time-independent domain. The advantage becomes more pronounced the further apart the fronts and pulses are in the original system. Interactions in the far field are treated by extrapolating the solutions of the subsystems. Second, the approach provides direct access to the shape and velocity of the pulses and fronts present in the original solution. It avoids any a-posteriori analysis of the numerical data in order to extract such information. The price to be paid for this advantage is the size of the system to be solved which grows with the number of pulses occuring.

The method turns out to be quite robust with respect to the choice of bump function which forms the building block of the decomposition. Moreover, several numerical tests confirm that the method is able to handle strong interactions that occur during collision or merging of pulses. Typically, after such collisions the dimension of our system is larger than necessary for decomposing the solution. Then the method still works and provides single components that add up to the correct solution and travel at a common speed or don't travel at all.

The theoretical foundation of the proposed method is still in its beginning. We prove that single waves of the given system provide a solution of our PDAE system in an asymptotic sense. Future work will require to show that the PDAE system is generally well-posed. Moreover, for the case of stable waves repelling each other one expects that the set of single waves forms an asymptotically stable equilibrium for the PDAE system.

Finally, the method is formulated in the abstract framework of equivariant evolution equations which encourages applications to much more general equations than the one-dimensional reaction diffusion systems discussed in this paper. First successful numerical tests are provided for the quintic-cubic Ginzburg Landau equation with a two-dimensional group of equivariances.

Appendix A. Proof of Theorem 4.2 (continued).

From the Lipschitz property of f and (4.12), (4.9), (4.10), (4.11), (4.14), (4.15), (4.17) we obtain the estimates:

$$
\begin{aligned}
I_1^b \leq & C \int_{-\infty}^{\gamma_1^+} |f(\sum_{k=1}^{N} \hat{w}_k(\xi + (c_j - c_k)t)) - f(w_1^-) + f(w_j^-) - f(w_j(\xi))|^2 d\xi \\
\leq & C \int_{-\infty}^{\gamma_1^+} \sum_{k=1}^{N} |w_k(\xi + (c_j - c_l)t) - w_k^-|^2 d\xi \\
\leq & C \int_{-\infty}^{\gamma_1^+} \sum_{k=1}^{N} e^{2\alpha(\xi + (c_j - c_k)t)} d\xi \leq C \int_{-\infty}^{\gamma_1^+} e^{2\alpha(\xi + (c_j - c_1)t)} d\xi \\
\leq & C e^{-2\alpha q(c_j - c_1)t}
\end{aligned}
$$

for $l \in \{1, \ldots, j-1\}$:

$$
\begin{aligned}
I_{1,l}^{1-} \leq & C \int_{\gamma_l^+}^{\gamma_l^0} \frac{\varphi(\xi)^2}{\varphi(\xi + (c_j - c_l)t)^2} d\xi \\
\leq & C \int_{\gamma_l^+}^{\gamma_l^0} e^{2((\beta_1 - \beta_0)\xi - \beta_0(c_j - c_l)t)} d\xi \leq C e^{2((\beta_0 - \beta_1)q - \beta_1)(c_j - c_l)t}
\end{aligned}
$$

for $l \in \{1, \ldots, j-1\}$:

$$
\begin{aligned}
I_{1,l}^{2-} \leq & C \int_{\gamma_l^0}^{\gamma_l^-} \frac{\varphi(\xi)^2}{\varphi(\xi + (c_j - c_l)t)^2} d\xi \\
\leq & C \int_{\gamma_l^0}^{\gamma_l^-} e^{2((\beta_1 + \beta_0)\xi + \beta_0(c_j - c_l)t)} d\xi \leq C e^{2((\beta_0 + \beta_1)q - \beta_1)(c_j - c_l)t}
\end{aligned}
$$

for $l \in \{1, \ldots, j-2\}$:

$$
\begin{aligned}
I_{1,l}^{3-} \leq & C \int_{\gamma_l^-}^{\gamma_{l+1}^+} |f(\sum_{k=1}^{N} \hat{w}_k(\xi + (c_j - c_k)t)) - f(w_l^+) + f(w_j^-) - f(w_j(\xi))|^2 d\xi \\
\leq & C \left[\int_{\gamma_l^-}^{\gamma_{l+1}^+} \sum_{k=1}^{l} |w_k(\xi + (c_j - c_k)t) - w_k^+|^2 d\xi \right. \\
& + \left. \int_{\gamma_l^-}^{\gamma_{l+1}^+} \sum_{k=l+1}^{N} |w_k(\xi + (c_j - c_k)t) - w_k^-|^2 d\xi \right] \\
\leq & C \left[\int_{\gamma_l^-}^{\gamma_{l+1}^+} \sum_{k=1}^{l} e^{-2\alpha(\xi + (c_j - c_k)t)} d\xi + \int_{\gamma_l^-}^{\gamma_{l+1}^+} \sum_{k=l+1}^{N} e^{2\alpha(\xi + (c_j - c_k)t)} d\xi \right] \\
\leq & C \left[\int_{\gamma_l^-}^{\gamma_{l+1}^+} e^{-2\alpha(\xi + (c_j - c_l)t)} + e^{2\alpha(\xi + (c_j - c_{l+1})t)} d\xi \right] \\
\leq & C \left[e^{-2\alpha q(c_j - c_l)t} + e^{-2\alpha q(c_j - c_{l+1})t} \right].
\end{aligned}
$$

We further obtain for $l \in \{j+1, \dots, N\}$:

$$
\begin{aligned}
I_{1,l}^{1+} &\leq C \int_{\gamma_l^-}^{\gamma_l^0} \frac{\varphi(\xi)^2}{\varphi(\xi + (c_j - c_l)t)^2} d\xi \\
&\leq C \int_{\gamma_l^-}^{\gamma_l^0} e^{2((-\beta_1 - \beta_0)\xi - \beta_0(c_j - c_l)t)} d\xi \leq C e^{2((\beta_0 + \beta_1)q - \beta_1)\gamma_l^0}
\end{aligned}
$$

for $l \in \{j+1, \dots, N\}$:

$$
\begin{aligned}
I_{1,l}^{2+} &\leq C \int_{\gamma_l^0}^{\gamma_l^+} \frac{\varphi(\xi)^2}{\varphi(\xi + (c_j - c_l)t)^2} d\xi \\
&\leq C \int_{\gamma_l^0}^{\gamma_l^+} e^{2((\beta_0 - \beta_1)\xi + \beta_0(c_j - c_l)t)} d\xi \leq C e^{2((\beta_0 - \beta_1)q - \beta_1)\gamma_l^0}
\end{aligned}
$$

and for $l \in \{j+1, \dots, N-1\}$:

$$
\begin{aligned}
I_{1,l}^{3+} &\leq C \int_{\gamma_l^+}^{\gamma_{l+1}^-} |f(\sum_{k=1}^N \hat{w}_k(\xi + (c_j - c_l)t)) - f(w_l^-) + f(w_j^-) - f(w_j(\xi))|^2 d\xi \\
&\leq C \left[\int_{\gamma_l^+}^{\gamma_{l+1}^-} |\sum_{k=1}^l |w_k(\xi + (c_j - c_k)t) - w_k^+|^2 d\xi \right. \\
&\quad \left. + \int_{\gamma_l^+}^{\gamma_{l+1}^-} \sum_{k=l+1}^N |w_k(\xi + (c_j - c_k)t) - w_k^-|^2 d\xi \right] \\
&\leq C \left[\int_{\gamma_l^+}^{\gamma_{l+1}^-} \sum_{k=1}^l e^{-2\alpha(\xi + (c_j - c_k)t)} d\xi + \int_{\gamma_l^+}^{\gamma_{l+1}^-} \sum_{k=l+1}^N e^{2\alpha(\xi + (c_j - c_k)t)} d\xi \right] \\
&\leq C \left[\int_{\gamma_l^+}^{\gamma_{l+1}^-} \sum_{k=1}^l e^{-2\alpha(\xi + (c_j - c_l)t)} d\xi + \int_{\gamma_l^+}^{\gamma_{l+1}^-} \sum_{k=l+1}^N e^{2\alpha(\xi + (c_j - c_{l+1})t)} d\xi \right] \\
&\leq C \left[e^{-2\alpha q \gamma_l^0} + e^{-2\alpha q \gamma_{l+1}^0} \right].
\end{aligned}
$$

Finally, we have

$$
\begin{aligned}
I_1^e &\leq C \int_{\gamma_N^+}^{\infty} |f(\sum_{k=1}^N \hat{w}_k(\xi + (c_j - c_k)t)) - f(w_N^+) + f(w_j^+) - f(w_j(\xi))|^2 d\xi \\
&\leq C \sum_{k=1}^N |w_k(\xi + (c_j - c_k)t) - w_k^+|^2 d\xi \leq C \int_{\gamma_N^+}^{\infty} \sum_{k=1}^N e^{-2\alpha(\xi + (c_j - c_k)t)} d\xi \\
&\leq C \int_{\gamma_N^+}^{\infty} e^{-2\alpha(\xi + (c_j - c_N)t)} d\xi \leq C e^{-2\alpha q(c_N - c_j)t}.
\end{aligned}
$$

For $j = 1$, the estimate of I_1 has fewer terms

$$
\begin{aligned}
I_1 \leq C & \left[\int_{-\infty}^{\gamma_2^-} |f(\sum_{k=1}^{N} \hat{w}_k(\xi_{k,1}^g)) - f(w_1(\xi))|^2 d\xi + \sum_{k=2}^{N} \int_{\gamma_k^-}^{\gamma_k^0} Q_1^g(\xi, t)^2 d\xi \right. \\
& + \sum_{k=2}^{N} \int_{\gamma_k^0}^{\gamma_k^+} Q_1^g(\xi, t)^2 d\xi + \sum_{k=2}^{N-1} \int_{\gamma_k^+}^{\gamma_{k+1}^-} |f(\sum_{k=1}^{N} \hat{w}_k(\xi_{k,1}^g)) - f(w_1(\xi))|^2 d\xi \\
& + \left. \int_{\gamma_N^+}^{\infty} |f(\sum_{k=1}^{N} \hat{w}_k(\xi_{k,1}^g)) - f(w_1(\xi))|^2 d\xi \right] \\
=: & \ I_1^c + \sum_{k=2}^{N} I_{1,k}^{1+} + \sum_{k=2}^{N} I_{1,k}^{2+} + \sum_{k=2}^{N-1} I_{1,k}^{3+} + I_1^e.
\end{aligned}
$$

$I_{1,k}^{1+}, I_{1,k}^{2+}, I_{1,k}^{3+}, I^e$ are estimated as before and for I_1^c we have

$$
\begin{aligned}
I_1^c \leq & C \int_{-\infty}^{\gamma_2^-} \sum_{k=2}^{N} e^{2\alpha(\xi + (c_1 - c_k)t)} d\xi \leq C \int_{-\infty}^{\gamma_2^-} e^{2\alpha(\xi + (c_1 - c_2)t)} d\xi \\
\leq & C e^{-2\alpha q(c_2 - c_1)t}.
\end{aligned}
$$

The estimate of I_1 for $j = N$ proceeds as follows:

$$
\begin{aligned}
I_1 \leq C & \left[\int_{-\infty}^{\gamma_1^+} |f(\sum_{k=1}^{N} \hat{w}_k(\xi_{k,N}^g)) - f(w_N(\xi)|^2 d\xi + \sum_{k=1}^{N-1} \int_{\gamma_k^+}^{\gamma_k^0} Q_N^g(\xi, t)^2 d\xi \right. \\
& + \sum_{k=1}^{N-1} \int_{\gamma_k^0}^{\gamma_k^-} Q_N^g(\xi, t)^2 d\xi + \sum_{k=1}^{N-2} \int_{\gamma_k^-}^{\gamma_{k+1}^+} |f(\sum_{k=1}^{N} \hat{w}_k(\xi_{k,N}^g)) - f(w_N(\xi)|^2 d\xi \\
& + \left. \int_{\gamma_{N-1}^-}^{\infty} |f(\sum_{k=1}^{N} \hat{w}_k(\xi_{k,N}^g)) - f(w_N(\xi)|^2 d\xi \right] \\
=: & \ I_1^b + \sum_{k=1}^{j-1} I_{1,k}^{1-} + \sum_{k=1}^{j-1} I_{1,k}^{2-} + \sum_{k=1}^{j-2} I_{1,k}^{3-} + I_1^c.
\end{aligned}
$$

The terms $I_1^b, I_{1,k}^{1-}, I_{1,k}^{2-}, I_{1,k}^{3-}$ are treated as before and for I_1^c we have:

$$
\begin{aligned}
I_1^c \leq & C \int_{\gamma_{N-1}^-}^{\infty} \sum_{k=1}^{N-1} e^{-2\alpha(\xi + (c_N - c_k)t)} d\xi \\
\leq & C \int_{\gamma_{N-1}^-}^{\infty} e^{-2\alpha(\xi + (c_N - c_{N-1})t)} d\xi \leq C e^{-2\alpha q(c_N - c_{N-1})t}.
\end{aligned}
$$

Finally, we estimate I_2. For $2 \le j \le N-1$ we partition into four terms:

$$I_2 \le C \left[\int_{-\infty}^{\gamma_{j-1}} |f(w_j(\xi))|^2 d\xi + \int_{\gamma_{j-1}}^{0} (1 - Q_j^g(\xi,t))^2 d\xi \right.$$

$$\left. + \int_0^{\gamma_{j+1}} (1 - Q_j^g(\xi,t))^2 d\xi + \int_{\gamma_{j+1}}^{\infty} |f(w_j(\xi))|^2 d\xi \right]$$

$$=: I_{2,1} + I_{2,2} + I_{2,3} + I_{2,4},$$

where

$$\gamma_k = q(c_k - c_j)t.$$

Employing the same estimates as above we find

$$I_{2,1} \le C \int_{-\infty}^{\gamma_{j-1}} |f(w_j(\xi)) - f(w_j^-)|^2 d\xi$$

$$\le C \int_{-\infty}^{\gamma_{j-1}} e^{2\alpha\xi} d\xi \le C e^{2\alpha\gamma_{j-1}}$$

$$I_{2,2} \le C \int_{\gamma_{j-1}}^{0} \frac{\left(\sum_{k=1}^{j-1} \varphi(\xi + (c_j - c_k)t) + \sum_{k=j+1}^{N} \varphi(\xi + (c_j - c_k)t) \right)^2}{\varphi(\xi)^2} d\xi$$

$$\le C \left[\int_{\gamma_{j-1}}^{0} \sum_{k=1}^{j-1} e^{-2(\beta_0+\beta_1)\xi - 2\beta_1(c_j - c_k)t} + \sum_{k=j+1}^{N} e^{2(-\beta_0+\beta_1)\xi + 2\beta_1(c_j - c_k)t} d\xi \right]$$

$$\le C \int_{\gamma_{j-1}}^{0} e^{-2(\beta_0+\beta_1)\xi - 2\beta_1(c_j - c_{j-1})t} + e^{2(-\beta_0+\beta_1)\xi + 2\beta_1(c_j - c_{j+1})t} d\xi$$

$$\le C(e^{2((\beta_0+\beta_1)q - \beta_1)(c_j - c_{j-1})t} + e^{2(\beta_0-\beta_1)q(c_j - c_{j-1})t - 2\beta_1(c_{j+1} - c_j)t})$$

$$I_{2,3} \le C \int_0^{\gamma_{j+1}} \frac{\left(\sum_{k=1}^{j-1} \varphi(\xi + (c_j - c_k)t) + \sum_{k=j+1}^{N} \varphi(\xi + (c_j - c_k)t) \right)^2}{\varphi(\xi)^2} d\xi$$

$$\le C \left[\int_0^{\gamma_{j+1}} \sum_{k=1}^{j-1} e^{2(\beta_0-\beta_1)\xi - 2\beta_1(c_j - c_k)t} + \sum_{k=j+1}^{N} e^{2(\beta_0+\beta_1)\xi + 2\beta_1(c_j - c_k)t} d\xi \right]$$

$$\le C \int_0^{\gamma_{j+1}} e^{2(\beta_0-\beta_1)\xi - 2\beta_1(c_j - c_{j-1})t} + e^{2(\beta_0+\beta_1)\xi + 2\beta_1(c_j - c_{j+1})t} d\xi$$

$$\le C \left[e^{2(\beta_0-\beta_1)\gamma_{j+1} - 2\beta_1(c_j - c_{j-1})t} + e^{2((\beta_0+\beta_1)q - \beta_1)(c_{j+1} - c_j)t} \right]$$

$$I_{2,4} \le C \int_{\gamma_{j+1}}^{\infty} |f(w_j(\xi)) - f(w_j^+)|^2 d\xi \le C \int_{\gamma_{j+1}}^{\infty} e^{-2\alpha\xi} d\xi \le C e^{-2\alpha\gamma_{j+1}}.$$

For $j=1$ we estimate I_2 as follows:

$$I_2 \le C \left[\int_{-\infty}^{-qt} |f(w_1(\xi))|^2 d\xi + \int_{-qt}^{0} (1 - Q_1^g(\xi,t))^2 d\xi \right.$$

$$\left. + \int_0^{\gamma_2} (1 - Q_1^g(\xi,t))^2 d\xi + \int_{\gamma_2}^{\infty} |f(w_1(\xi))|^2 d\xi \right]$$

$$=: I_{2,1} + I_{2,2} + I_{2,3} + I_{2,4}.$$

$I_{2,3}$ and $I_{2,4}$ are estimated as before and for $I_{2,1}$ and $I_{2,2}$ we obtain:

$$I_{2,1} \leq C \int_{-\infty}^{-qt} |f(w_1(\xi)) - f(w_1^-)|^2 d\xi \leq C \int_{-\infty}^{-qt} e^{2\alpha_1 \xi} d\xi \leq C e^{-2\alpha_1 qt}$$

$$I_{2,2} \leq C \int_{-qt}^{0} \frac{\sum_{k=2}^{N} \varphi(\xi + (c_1 - c_k)t)^2}{\varphi(\xi)^2} d\xi \leq C \int_{-qt}^{0} \sum_{k=2}^{N} e^{2(-\beta_0 + \beta_1)\xi + 2\beta_1(c_1 - c_k)t} d\xi$$

$$\leq C \int_{-qt}^{0} e^{2(-\beta_0 + \beta_1)\xi + 2\beta_1(c_1 - c_2)t} d\xi \leq C(e^{2(\beta_0 - \beta_1)qt - 2\beta_1(c_2 - c_1)t}).$$

Similarly, we find for $j = N$:

$$I_2 \leq C \left[\int_{-\infty}^{\gamma_{N-1}} |f(w_N(\xi))|^2 d\xi + \int_{\gamma_{N-1}}^{0} (1 - Q_N^g(\xi,t))^2 d\xi \right.$$

$$+ \left[\int_0^{qt} (1 - Q_N^g(\xi,t))^2 d\xi + \int_{qt}^{\infty} |f(w_N(\xi))|^2 d\xi \right]$$

$$=: I_{2,1} + I_{2,2} + I_{2,3} + I_{2,4}.$$

$I_{2,1}$ and $I_{2,2}$ are as before and $I_{2,3}$, $I_{2,4}$ satisfy:

$$I_{2,3} \leq C \int_0^{qt} \frac{\sum_{k=1}^{N-1} \varphi(\xi + (c_N - c_k)t)^2}{\varphi(\xi)^2} d\xi \leq C \int_0^{qt} \sum_{k=1}^{N-1} e^{2(\beta_0 - \beta_1)\xi - 2\beta_1(c_N - c_k)t} d\xi$$

$$\leq C \int_0^{qt} e^{2(\beta_0 - \beta_1)\xi - 2\beta_1(c_N - c_{N-1})t} d\xi \leq C e^{2(\beta_0 - \beta_1)qt - 2\beta_1(c_N - c_{N-1})t}$$

$$I_{2,4} \leq C \int_{qt}^{\infty} |f(w_N(\xi)) - f(w_N^+)|^2 d\xi \leq C \int_{qt}^{\infty} e^{-2\alpha\xi} d\xi \leq C e^{-2\alpha qt}.$$

REFERENCES

[1] H. Airault. Équations asymptotiques pour des cas spéciaux de l'équation de Nagumo. *C. R. Acad. Sci. Paris Sér. I Math.*, 301(6):295–298, 1985.

[2] C. Anderson and C. Greengard. On vortex methods. *SIAM J. Numer. Anal.*, 22(3):413–440, 1985.

[3] W.-J. Beyn and V. Thümmler. Freezing solutions of equivariant evolution equations. *SIAM Journal on Applied Dynamical Systems*, 3(2):85–116, 2004.

[4] W.-J. Beyn and V. Thümmler. Phase conditions, Symmetries, and PDE Continuation. In B. Krauskopf, H. Osinga, and J. Galan-Vioque, editors, *Numerical Continuation Methods for Dynamical Systems*, Series in Complexity, pages 301–330. Springer, 2007.

[5] Comsol Multiphysics 3.3, 2007. Comsol Inc., www.comsol.com.

[6] J. W. Evans, N. Fenichel, and J. A. Feroe. Double impulse solutions in nerve axon equations. *SIAM J. Appl. Math.*, 42(2):219–234, 1982.

[7] S. A. J. Nagumo and S. Yoshizawa. An active pulse transmission line simulating nerve axon. In *Proceedings of the IRE*, volume 50, pages 2061–2070, 1962.

[8] A. J. Majda and A. L. Bertozzi. *Vorticity and incompressible flow*, volume 27 of *Cambridge Texts in Applied Mathematics*. Cambridge University Press, Cambridge, 2002.

[9] R. M. Miura. Accurate computation of the stable solitary waves for the FitzHugh-Nagumo equations. *Journal of Mathematical Biology*, 13:247–269, 1982.

[10] J. D. Murray. *Mathematical Biology*, volume 19 of *Biomathematics*. Springer-Verlag, Berlin, second edition, 1993.

[11] S. Nii. A topological proof of stability of N-front solutions of the FitzHugh-Nagumo equations. *J. Dynam. Differential Equations*, 11(3):515–555, 1999.

[12] C. W. Rowley, I. G. Kevrekidis, J. E. Marsden, and K. Lust. Reduction and reconstruction for self-similar dynamical systems. *Nonlinearity*, 16(4):1257–1275, 2003.

[13] B. Sandstede. Stability of multiple-pulse solutions. *Trans. Amer. Math. Soc.*, 350(2):429–472, 1998.

[14] B. Sandstede. Stability of N-fronts bifurcating from a twisted heteroclinic loop and an application to the FitzHugh-Nagumo equation. *SIAM J. Math. Anal.*, 29(1):183–207 (electronic), 1998.

[15] B. Sandstede. Stability of travelling waves. In *Handbook of dynamical systems, Vol. 2*, pages 983–1055. North-Holland, Amsterdam, 2002.

[16] B. Sandstede and A. Scheel. Gluing unstable fronts and backs together can produce stable pulses. *Nonlinearity*, 13(5):1465–1482, 2000.

[17] A. Scheel and J. D. Wright. Colliding dissipative pulses - the shooting manifold. Preprint, University of Minnesota, 2006.

[18] O. Thual and S. Fauve. Localized structures generated by subcritical instabilities. *J. Phys. France*, 49:1829–1833, 1988.

[19] V. Thümmler. *Numerical Analysis of the method of freezing traveling waves*. PhD thesis, Dept. of Mathematics, Bielefeld University, 2005.

[20] V. Thümmler. Asymptotic stability of frozen relative equilibria. Preprint no. 06-30 of the CRC 701, Bielefeld University (to appear in JDDE), 2006.

[21] W. van Saarloos and P. C. Hohenberg. Fronts, pulses, sources and sinks in generalized complex Ginzburg-Landau equations. *Phys. D*, 56(4):303–367, 1992.

[22] E. Yanagida and K. Maginu. Stability of double-pulse solutions in nerve axon equations. *SIAM J. Appl. Math.*, 49(4):1158–1173, 1989.

[23] S. Zelik and A. Mielke. Multi-pulse evolution and space-time chaos in dissipative systems. Preprint 1093, Weierstraß-Institut für Angewandte Analysis und Stochastik, 2006.